

U.S. DEPARTMENT OF THE INTERIOR  
U.S. GEOLOGICAL SURVEY

**Lake Baikal - 1992**  
**Processing of Multichannel Seismic Reflection Data**

by  
W.F. Agena, M.W. Lee<sup>1</sup>, J.J. Miller<sup>1</sup>, and D.R. Hutchinson<sup>2</sup>

U.S. Geological Survey  
Open-File Report 94-263

This report is preliminary and has not been reviewed for conformity with U.S. Geological Survey editorial standards and stratigraphic nomenclature. Any use of trade names is for descriptive purposes only and does not imply endorsement by the U.S. Geological Survey.

<sup>1</sup>U.S. Geological Survey, Box 25046, MS 960, DFC, Denver, CO 80225

<sup>2</sup>U.S. Geological Survey, Woods Hole, MA 02543

## TABLE OF CONTENTS

Introduction .....	2
Acknowledgements.....	2
Acquisition .....	2
General Processing Sequence.....	5
Data Characteristics and Problems.....	5
Data Archiving .....	8
References .....	11
Appendix A - Tape Archive Tables.....	12
Appendix B - Profiles.....	18

## FIGURES

Figure 1 - 1992 Lake Baikal MCS profiles.....	3
Figure 2 - Processing Flow for the 1992 Lake Baikal MCS data set.....	6
Figure 3 - Velocity analysis on CMPS without time delay.....	9
Figure 4 - Velocity analysis on CMPS with time delay corrections .....	10

## TABLE

Table 1 - Acquisition Parameters.....	4
---------------------------------------	---

## INTRODUCTION

During August and September of 1992, an international cooperative effort was undertaken to investigate the world's deepest and most voluminous fresh water body, Lake Baikal in Siberia, using multichannel seismics (MCS). Lake Baikal is approximately 600 km long and 50 km wide and lies in the central region of one of the world's most active continental rift systems. It is bounded on the northwest by the stable Siberian craton, and to the south and east by active fold belts of Mongolia. The lake contains three bathymetric basins (Southern, Central, and Northern) separated by two bathymetric sills, Selenga Delta on the southwest, and Academician Ridge in the northeast. An earlier reconnaissance multichannel seismics survey in the lake provided information on the general depositional and tectonic framework of the sub basins (Hutchinson et al., 1992a, 1992b). For the 1992 survey, seismic profiles were concentrated on the two sills (Selenga Delta and Academician Ridge) separating the three sub basins. A map showing the locations of the profiles is shown in Figure 1.

The purpose of this report is to describe the processing and archiving of the multichannel seismics data collected in the 1992 field season. Because earlier reports have summarized the acquisition and hardware configuration used in the data collection (Nichols et al., 1992; Klitgord et al., 1993), this report only summarizes acquisition information that is relevant to understanding the processing strategy for the data.

## ACKNOWLEDGMENTS

We thank Dave Taylor and Chris Schneider for constructive reviews of an earlier version of this report. The 1992 MCS data were processed by members of the Geophysics Group from the Branch of Petroleum Geology in Denver, CO, using DISCO software and processing modules developed in house. Funding for the field work was jointly provided by the U.S. Geological Survey, the U.S. National Science Foundation, and the Russian Academy of Sciences.

## ACQUISITION

The acquisition systems used during the 1992 experiment consisted of U.S. and Russian equipment. The source for all but one line was a 10-gun Russian airgun array with a total volume of 1675 in<sup>3</sup> (24 l). The one exception, line 17A, was shot with a two-gun array totaling 7329 in<sup>3</sup> (60 l). The receiver was a 2400-m long Russian hydrophone streamer consisting of 96 channels spaced 25-m apart. For seven lines in the narrowest part of the lake, lines 12, 14, 16, 18, 20, 22, and 24, the streamer was reduced to 1200-m long (48 channels spaced 25-m apart). A U.S.-built DFS-V computer provided the acquisition system; data were recorded with a 4-ms sampling rate in SEG-B format on 9-Track magnetic tapes. Table 1 gives tabulated information about specific acquisition parameters for each line. Details about equipment hardware and cruise narratives are given in Nichols et al. (1992) and Klitgord et al. (1993).

Navigation was by Global Positioning Satellite (GPS) and was recorded independently from the multichannel data. Shots were fired by time, with the shot interval adjusted to give nominal 50-meter shots depending on the ship's speed. For a ship's speed of 4.0 to 4.5 kts, the shot interval varied between 25 and 23 seconds (Klitgord et al. 1993). GPS fixes were digitally recorded every 10 seconds; the record number from the DFS V was logged with the navigation every 15 minutes, or about every 35 shots, depending on the speed of the ship and the firing interval. In post cruise processing, the 15-minute shot numbers were then interpolated across the 10-second positional fixes to yield final navigation locations for each shot.

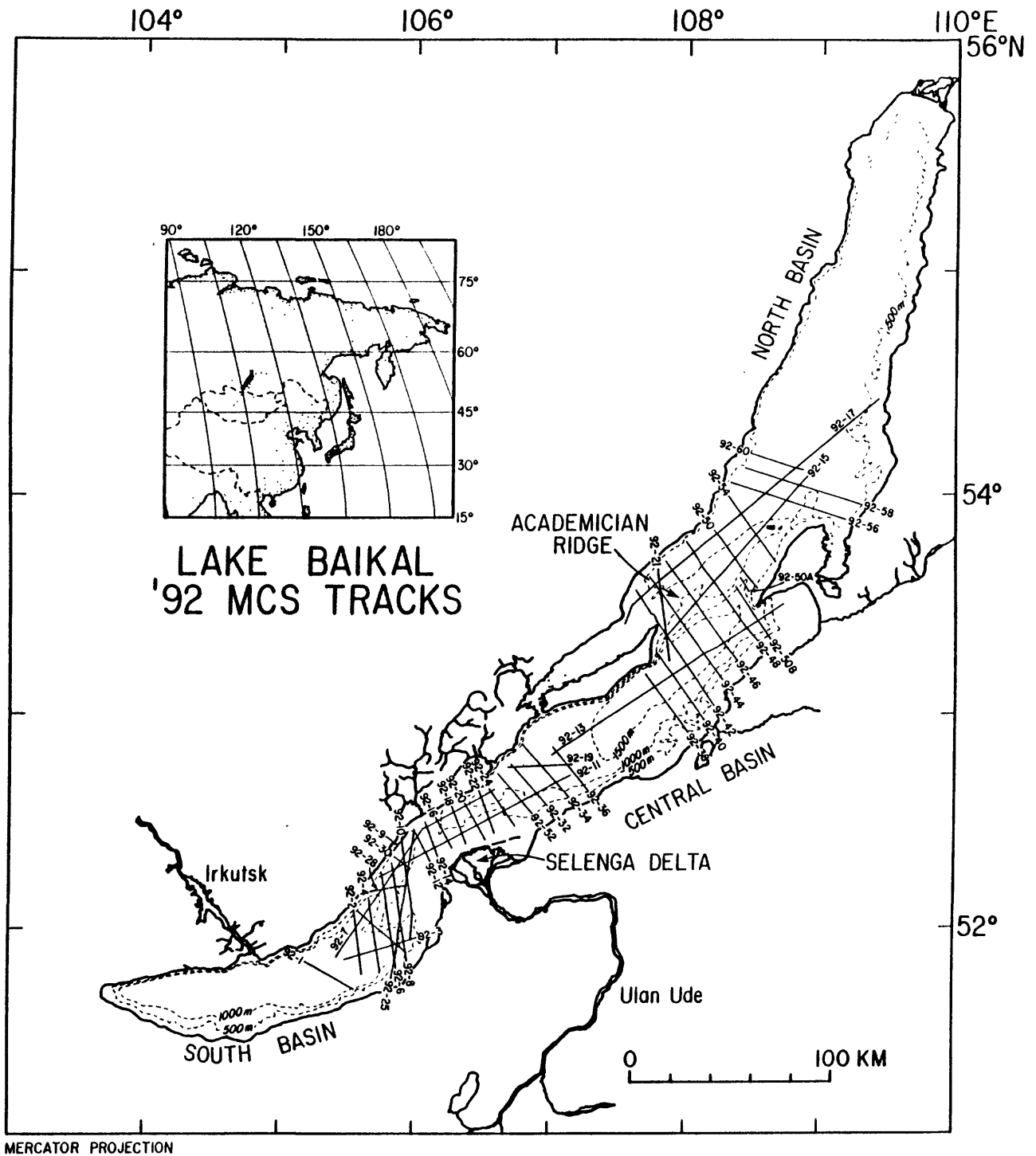


Figure 1 - 1992 Lake Baikal MCS profiles (From Klitgord et al.)

Line	Length (Km)	First Shot	Last Shot	Source Volume (in <sup>3</sup> ) ***	Cable Length (m)	Channels	Near Offset (m)	Record Length (s)	Fold	Migrated
92-1	28.7	1	559	1675	2400	96	495	7/8	24	
92-2	34.4	1	683	1675	2400	96	495	8	24	
92-3	17.7	1	332	1675	2400	96	495	8	24	
92-3A	25.7	1	495	1675	2400	96	495	8	24	
92-4	41.5	1	785	1675	2400	96	495	8	24	YES
92-6	50.7	1	989	1675	2400	96	495	8	24	YES
92-7	118.2	1	2430	1675	2400	96	495	8	24	YES
92-8	52.3	1	1002	1675	2400	96	495	8	24	YES
92-9	10.2	2	209	1675	2400	96	495	8	24	
92-10	32.9	1	612	1675	2400	96	495	8	24	
92-10A	39.8	268	1082	1675	2400	96	495	8	24	YES
92-11	108.0	1	2137	1675	2400	96	400	9	24	YES
92-12	18.2	1	389	1675	1200	48	500	8	12	YES
92-13	137.3	1	2589	1675	2400	96	400	9	24	YES
92-14	19.9	1	445	1675	1200	48	500	8	12	YES
92-15	117.5	1	2055	1675	2400	96	400	9	24	YES
92-16	17.4	1	375	1675	1200	48	500	8	12	YES
92-17*	167.3	4	3269	1675	2400	96	400	9	24	YES
92-17A**	163.9	5	641	7320	2400	96	400	16	6	
92-18	20.5	1	419	1675	1200	48	500	8	12	YES
92-19	32.5	1	614	1675	2400	96	400	9	24	
92-20	20.7	1	412	1675	1200	48	500	8	12	YES
92-21	46.2	1	839	1675	2400	96	400	9	24	
92-22	23.0	7	447	1675	1200	48	500	8	12	YES
92-23	11.1	1	214	1675	2400	96	400	9	24	
92-24	23.3	6	608	1675	1200	48	500	8	12	
92-25	79.4	1	1512	1675	2400	96	400	9	24	YES
92-26	35.1	1	682	1675	2400	96	495	8	24	
92-28	19.4	1	422	1675	2400	96	495	8	24	
92-30	9.9	1	174	1675	2400	96	495	8	24	
92-32	26.7	1	515	1675	2400	96	400	9	24	
92-34	35.0	1	680	1675	2400	96	400	9	24	
92-36	28.2	1	525	1675	2400	96	400	9	24	
92-38	37.2	3	727	1675	2400	96	400	8	24	YES
92-40	15.5	2	287	1675	2400	96	400	9	24	YES
92-40A	32.4	241	860	1675	2400	96	400	9	24	YES
92-42	70.0	1	1321	1675	2400	96	400	9	24	YES
92-44	62.9	1	1202	1675	2400	96	400	9	24	YES

\* One field reel on line 17 was blank, resulting in no data for SP 2684 to 2757

\*\* Line 17A was called 17OB during processing

\*\*\* 1675 in<sup>3</sup> - 10-gun airgun array, shot interval = 23-25 seconds (≈ 50m)  
7320 in<sup>3</sup> 2-gun array (60-liters each), shot interval = 2 minutes (≈ 200-250m)

Table 1 - Acquisition Parameters

Line	Length (Km)	First Shot	Last Shot	Source Volume (in <sup>3</sup> )	Cable Length (m)	Channels	Near Offset (m)	Record Length (s)	Fold	Migrated
92-46	61.0	1	1180	1675	2400	96	400	9	24	YES
92-48	60.2	2	1110	1675	2400	96	400	9	24	YES
92-50	32.9	1	680	1675	2400	96	400	9	24	YES
92-50A	7.4	1	148	1675	2400	96	400	9	24	YES
92-50B	31.7	1	635	1675	2400	96	400	9	24	YES
92-52	26.1	1	495	1675	2400	96	400	9	24	
92-54	40.0	1	780	1675	2400	96	400	7	24	YES
92-56	58.2	1	1143	1675	2400	96	400	7	24	YES
92-58	59.3	1	1138	1675	2400	96	400	7	24	YES
92-60	28.9	1	545	1675	2400	96	400	8	24	

Table 1 - Acquisition Parameters (cont.)

## GENERAL PROCESSING SEQUENCE

The processing sequence for the 1992 data set followed conventional pre-stack processing methods and is summarized in figure 2. Table 1 shows that 35 lines were shot with 24-fold common mid-point (CMP) coverage, 7 were shot with 12-fold coverage, and 1 was shot with 6-fold coverage. After corrections for geometry problems (discussed in the next section) were applied, the shot ordered data were edited, resampled at 6 milliseconds (ms) and sorted into CMP order. A 500 ms automatic gain control (AGC) operator and spiking deconvolution were then applied to the data and velocities were analyzed every 200 CMPs (2.5 km) in areas with little or no geologic structure, and every 50 or 100 CMPs (.625 & 1.25 km respectively) in areas with structure. After velocities were picked, normal moveout (NMO) was applied and the data were muted and stacked. Post stack processing included applying a 1000 ms AGC operator, a second-zero crossing predictive deconvolution, and on 26 lines, cascaded migrations. Larner and Beasley (1987) described the method of using cascaded migrations to improve the accuracy of finite-difference migrations in areas with steeply dipping events.

## DATA CHARACTERISTICS AND PROBLEMS

In processing this data set, two major problems existed: (1) lost shots either at tape changes or on bad tapes; and (2) time delay inaccuracies.

The first problem, regarding lost shots, was caused by two hardware failures. One of the two tape drives on the acquisition computer malfunctioned half way through the cruise. Prior to its complete failure, numerous shots were lost at tape changes when the drive failed to start smoothly. The maximum number of lost shots was generally only a few, but did reach a maximum of about 20. After recording with the malfunctioning transport was discontinued, the remaining tape unit had to be manually unloaded before rewind, then reloaded with a fresh tape at tape changes, resulting in about 2-shots lost every tape change. These lost shots were inserted as zeroed gathers at demultiplex. Generally, the slight fold reduction caused by the missing shots caused no obvious loss in data quality.

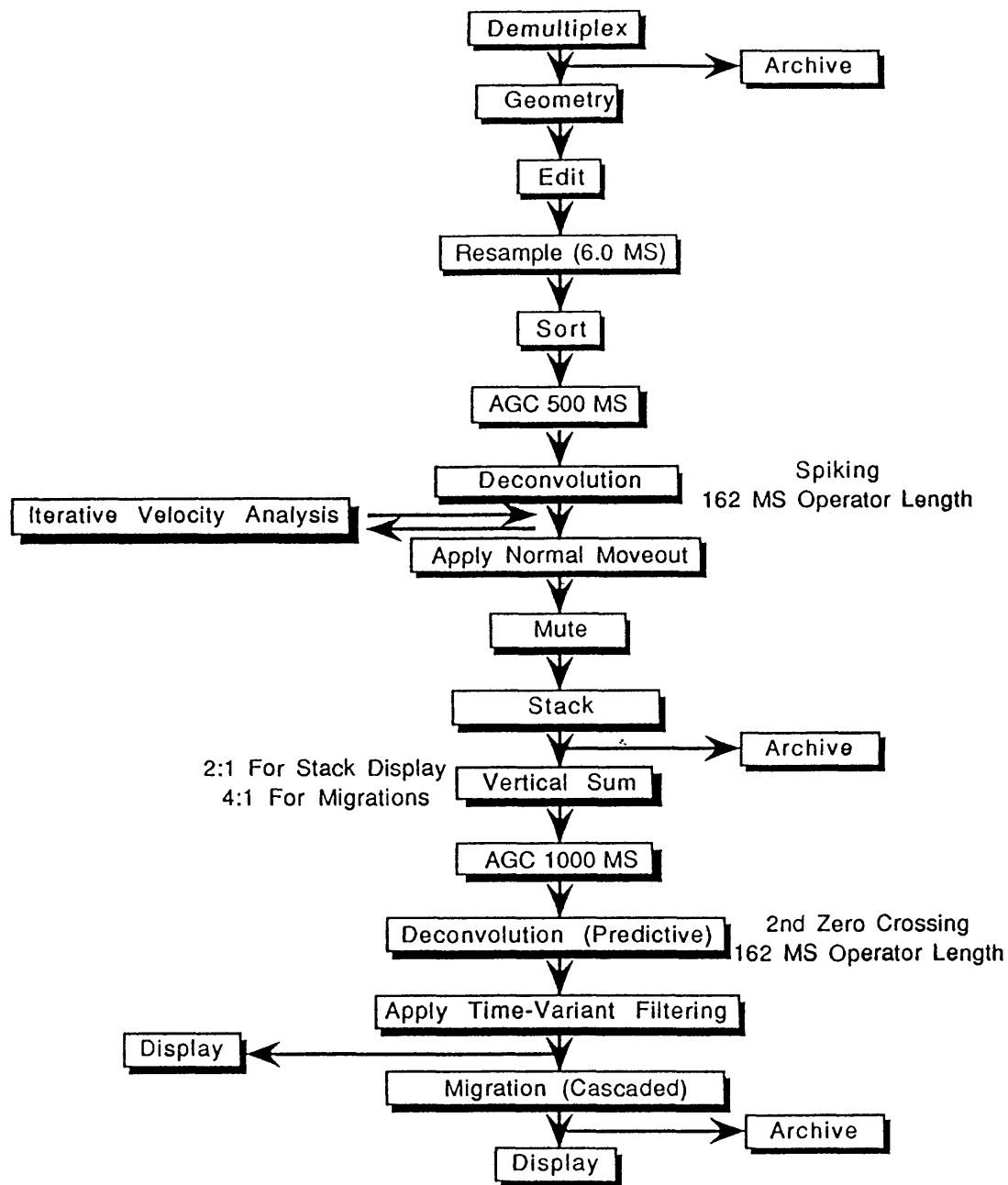


Figure 2 - Processing Flow for the 1992 Lake Baikal MCS data set

The other reason for lost shots involved poor quality 9T tapes that caused an unusually large number of parity errors and missed records during the first part of the field program. This second malfunction, once understood, was rectified by using another brand of tapes available on the cruise. Not all of the lost shots from poor tape quality were rigorously logged in the observers notes. Consequently, zeroed shots were occasionally added during the processing to allow for obvious misalignments in the water bottom arrival on successive shots. These zeroed shots generally numbered a few.

The problem of the lost shots affected the whole cruise: in the first half, because of bad tapes and an erratic tape drive, and in the second half because of only one tape drive available for recording.

A consequence of the lost shots is that there are not always shot numbers assigned to the missing shots and the interval between 100 shots is not always exactly 5 km. This occurs because the shot numbers were calibrated exactly to the record numbers on the DFS V tapes. Using the example of two missed shots during tape changes, the shot number on the full tape and the subsequent shot number on the new tape are successive even though two gun firings occurred between the two record (i.e., shot) numbers. This means that whenever a tape change occurs, the interval between successive shot numbers is 150 m, even though the guns continued to fire every 50 m. The distance is larger when more firings occurred or had to be inserted because of the bad tapes. This explains the non-regular spacing of the 100-shot labels on the final MCS profiles.

The second problem involved incorrect absolute zero times on some of the lines. During processing, we discovered that a time shift of up to 50 ms existed between the first water bottom multiple and twice the arrival time of the lake floor. This was variable between lines and sometimes changed within an individual line. This delay can be corrected by applying an appropriate static shift to the shot gather. However, calculating the appropriate static shift is time consuming because it involves iterative static shifts and velocity analyses along the line. Consequently, we only corrected this residual timing error on a few key lines which needed accurate velocities for further analysis (B92-1, 2, 4, 6, 40, & 40A). Because stacking velocity depends on the apparent hyperbolic moveout times, the seismic data can still be accurately stacked even when bulk timing errors exist.

The error caused by these timing uncertainties in absolute zero can be estimated. The error is important for calculations of interval velocity, because interval velocity is based on absolute stacking velocity (i.e., RMS velocity) using the Dix equation (Dix, 1955). If the stacking velocities are incorrect due to timing errors, then the interval velocity will also be incorrect, even though the data stack optimally with the incorrect stacking velocities.

Stacking velocities can be derived from the normal moveout (NMO) equation:

$$V_s^2 = \frac{X^2}{2T_o T_{nmo}} \quad (1)$$

where  $V_s$  is stacking velocity,  $X$  is offset,  $T_o$  is zero-offset time, and  $T_{nmo}$  is NMO time for offset  $x$ . Differentiating Equation (1) under constant NMO time, the following equation can be derived:

$$\frac{\Delta V_s}{V_s} = \frac{-\Delta T_o}{2T_o} \quad (2)$$

where  $\Delta V_s$  is the uncertainty in the stacking velocity and  $\Delta T_o$  is the uncertainty in the zero-offset time.

If there is a 50 ms time delay error in a CMP gather, the apparent stacking velocity has a  $-50 / 2000$  or 2.5% error for an arrival at 1000 ms. The earlier arrival times have more error in the stacking velocities. For portions of Line 8 where water bottom time is about 200 ms, the error in stacking velocities is about 12%. An example of an actual velocity analysis is given in Figures 3 and 4. Figure 3 shows the velocity analysis without a time delay correction and Figure 4 shows the velocity analysis with the correction of 50 ms time delay. The strong trough near the water bottom around 1600 ms stacks in at about 1400 m/s in Figure 3, versus about 1420 m/s in Figure 4. This amount of error is very close to 1.6% predicted by Equation (2). To facilitate processing and for consistency, we decided to process this data set using 1400 m/s to stack the water bottom. For most of the data, the amount of error this introduced was less than 2.0%.

The Dix formula for interval velocity can be written as follows:

$$\overline{V}_i^2 = \frac{V_{i+1}^2 T_{i+1} - V_i^2 T_i}{T_{i+1} - T_i} \quad (3)$$

where  $V_i$  is the interval velocity in the  $i$ -th layer and  $T_i$  is the arrival time to the  $i$ -th layer. Differentiating Equation (3) with respect to interval velocity and stacking velocity, we can derive the following equation relating the uncertainty of interval velocity to the uncertainty in the stacking velocity.

$$\frac{\Delta \overline{V}_i}{\overline{V}_i} = \frac{-\Delta T_o}{2T_{i+1}} \left\{ \frac{1 - \frac{V_i^2}{V_{i+1}^2}}{1 - \frac{V_i^2 T_i}{V_{i+1}^2 T_{i+1}}} \right\} \quad (4)$$

Equation (4) indicates that the maximum error in the interval velocity from the erroneous stacking velocity is almost the same as the error in the stacking velocity and this occurs when  $T_i$  and  $T_{i+1}$  are close to each other. Equation (4) also shows that in most cases, the error in the interval velocity is less than the error in the stacking velocity, because the quantity inside the parentheses is less than 1.

Let's assume that the true stacking velocity for water is 1420 m/s and the stacking velocity for the second layer, whose two-way traveltime thickness is 100 ms, is 1450 m/s. Let's also assume that there is a 50 ms time delay in the CMP gather and the water depth in two-way traveltime is 1000 ms. Then the stacking velocity analysis gives 1384 m/s for the water and 1417 m/s for the second layer, which corresponds to stacking velocity errors of 2.5% and 2.3% respectively. If we put these numbers into Equation (4) the error in the interval velocity is about 0.8%. When the water depth is about 500 ms, then the error in stacking velocity is 5% for the water and 4% for the second layer. However, the error in the interval velocity is only about 1%. Thus, for a large majority of the lines processed in this survey, where two-way traveltimes to the water bottom are greater than 500 ms, the interval velocities derived from the erroneous stacking velocities are still accurate to within a few percent.

## DATA ARCHIVING

All the data tapes were archived in the industry standard SEG-Y format and are currently being stored in the tape library at the U.S. Geological Survey's processing center in Denver. The

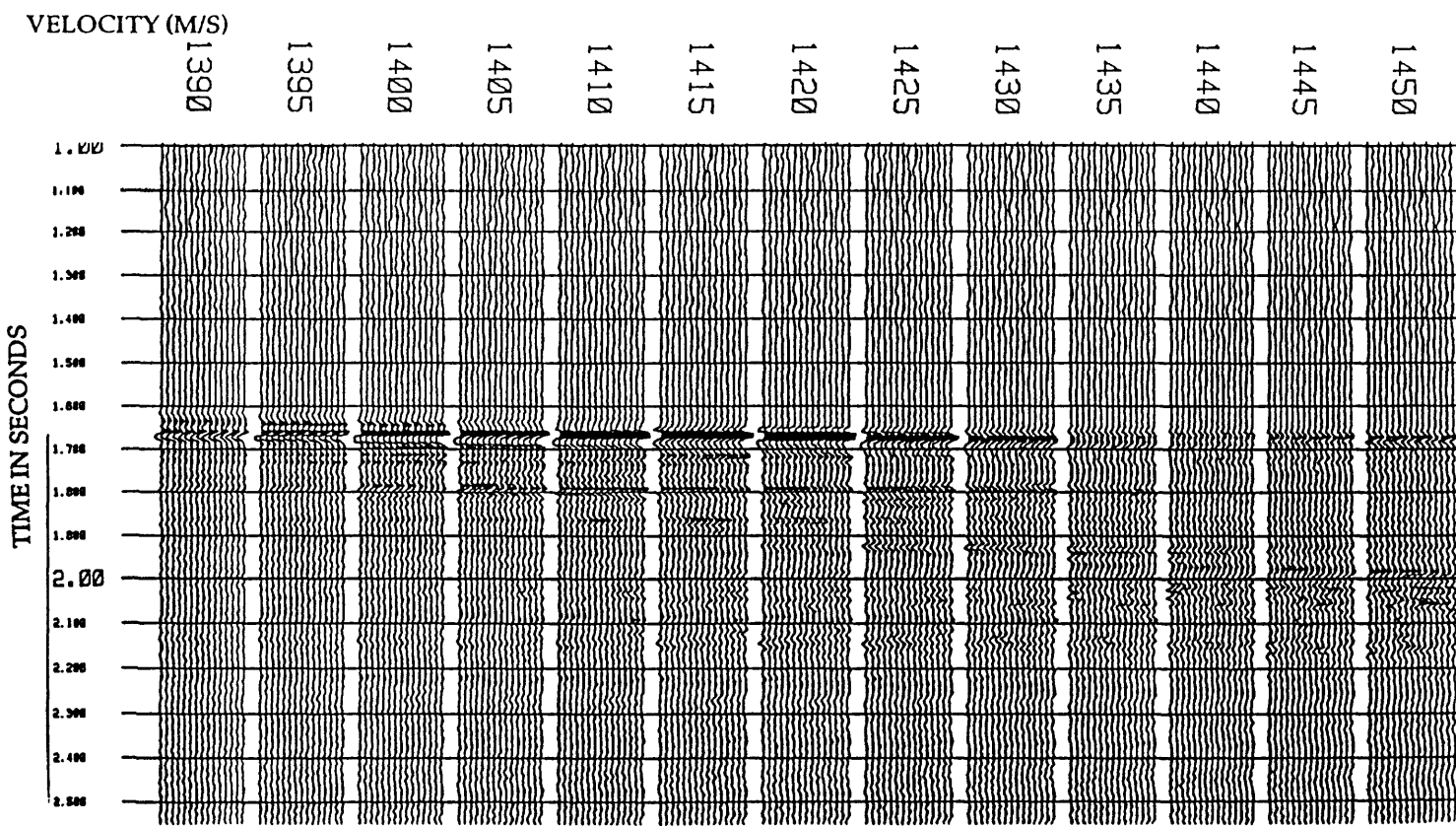


Figure 3 - Velocity analysis on CMPS without time delay

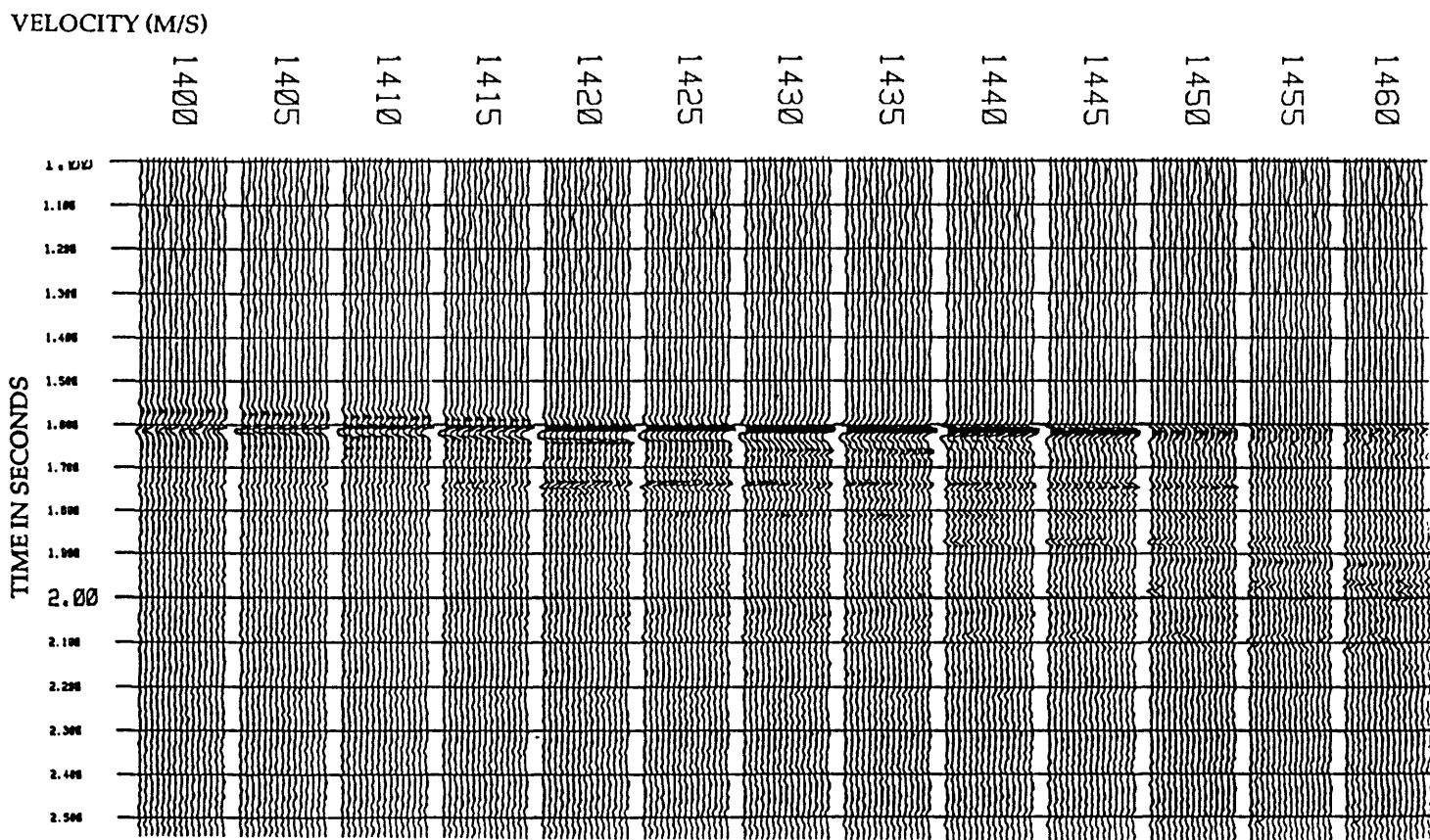


Figure 4 - Velocity analysis on CMPS with time delay corrections

demultiplexed field tapes are archived on 6250 bits per inch (BPI) 9-track magnetic tapes. SEG-Y images of final stacked and migrated data were written to 8-mm tapes using the UNIX "tar" format. The tables in Appendix A summarize the tape archive information. Slot numbers in the tables refer to U.S. Geological Survey tape library database identification numbers. Small scale plots of final stacked sections are included in Appendix B and all times shown are two-way traveltimes.

## REFERENCES

- Dix, C.H., 1955, Seismic velocities from surface measurements: *Geophysics*, v.20, p.68-86.
- Hutchinson, D.R., Golmshtok, A.J., Zonenshain, L.P., Moore, T.C., Scholz, C.A., and Klitgord, K.D., 1992, Depositional and tectonic framework of the rift basins of Lake Baikal from multichannel seismic data: *Geology*, v. 20, p. 589-592.
- Hutchinson, D.R., Lee, M.W., Agena, W.F., Golmshtok, A.J., Moskalenko, V.N., Karapetov, K., Coleman, D.F., and Akentiev, L., 1992, Processing of Lake Baikal Marine Multichannel Seismic Reflection Data: U.S. Geological Survey Open-file Report 92-243, 57p.
- Klitgord, K.D., Golmshtok, A.J., Scholz, C.A., Akentiev, L., Nichols, D., Schneider, C., McGill, J., Foster, D., and Unger, D., 1993, Seismic Survey of Lake Baikal, Siberia, Cruise Report: RV Balkash 25 August to 25 September, 1992: U.S. Geological Survey Open-file Report 93-201, 24p.
- Larner, K., and Beasley, C., 1987, Cascaded Migrations: improving the accuracy of finite-difference migration: *Geophysics*, v. 52, p. 618-643.
- Nichols, D.R., Miller, G., and Akentiev, L., 1992, Seismic Survey of Lake Baikal, Siberia: operational technical summary for R/V Balkhash and R/V Titov, 15 August to 30 September, 1992: U.S Geological Survey Open-file Report OF-92-693, 21p.
- Zonenshain, L.P., and Savostin, L.A., 1981, Geodynamics of the Baikal rift zone and plate tectonics of Asia, *Tectonophysics*, 76, p.1-45.

## APPENDIX A - TAPE ARCHIVE TABLES

Line	Slot	Reel	File	Type
B92-1	4317	B2-01-01	1-169	DEMUX
B92-1	8929	B2-01-02	169-338	DEMUX
B92-1	8930	B2-01-03	338-510	DEMUX
B92-1	8931	B2-01-04	510-559	DEMUX
B92-2	8932	B2-02-01	1-154	DEMUX
B92-2	8933	B2-02-02	154-320	DEMUX
B92-2	8934	B2-02-03	320-477	DEMUX
B92-2	8935	B2-02-04	477-552	DEMUX
B92-2	8936	B2-02-05	553-643	DEMUX
B92-3	8937	B2-03-01	2-180	DEMUX
B92-3	8938	B2-03-02	180-351	DEMUX
B92-3	8939	B2-03-03	351-358	DEMUX
B92-3A	8940	B2-3A-01	1-174	DEMUX
B92-3A	8941	B2-3A-02	174-344	DEMUX
B92-3A	8942	B2-3A-03	344-496	DEMUX
B92-4	8943	B2-04-01	1-159	DEMUX
B92-4	8944	B2-04-02	159-318	DEMUX
B92-4	8945	B2-04-03	318-477	DEMUX
B92-4	8946	B2-04-04	477-636	DEMUX
B92-4	8947	B2-04-05	636-636	DEMUX
B92-4	8948	B2-04-06	637-788	DEMUX
B92-6	8949	B2-06-01	1-175	DEMUX
B92-6	8950	B2-06-02	175-345	DEMUX
B92-6	8951	B2-06-03	345-516	DEMUX
B92-6	8952	B2-06-04	516-686	DEMUX
B92-6	8953	B2-06-05	686-733	DEMUX
B92-6	8954	B2-06-06	740-925	DEMUX
B92-6	8955	B2-06-07	925-989	DEMUX
B92-7	8956	B2-07-01	1-175	DEMUX
B92-7	8957	B2-07-02	175-349	DEMUX
B92-7	8958	B2-07-03	349-524	DEMUX
B92-7	8959	B2-07-04	524-698	DEMUX
B92-7	8960	B2-07-05	698-874	DEMUX
B92-7	8961	B2-07-06	874-1049	DEMUX
B92-7	8962	B2-07-07	1049-1198	DEMUX
B92-7	8963	B2-07-08	1201-1378	DEMUX
B92-7	8964	B2-07-09	1378-1553	DEMUX
B92-7	8965	B2-07-10	1553-1728	DEMUX
B92-7	8966	B2-07-11	1728-1903	DEMUX
B92-7	8967	B2-07-12	1903-2077	DEMUX
B92-7	8968	B2-07-13	2077-2256	DEMUX
B92-7	8969	B2-07-14	2256-2430	DEMUX
B92-7	13111	B2-07-15	2430-2430	DEMUX
B92-8	13112	B2-08-01	2-177	DEMUX
B92-8	13113	B2-08-02	177-351	DEMUX
B92-8	13114	B2-08-03	351-525	DEMUX

Line	Slot	Reel	File	Type
B92-8	13115	B2-08-04	525-702	DEMUX
B92-8	13116	B2-08-05	702-862	DEMUX
B92-8	13117	B2-08-06	863-1002	DEMUX
B92-9	13118	B2-09-01	2-172	DEMUX
B92-9	13119	B2-09-02	172-209	DEMUX
B92-10	13120	B2-10-01	1-173	DEMUX
B92-10	13121	B2-10-02	173-347	DEMUX
B92-10	13122	B2-10-03	347-517	DEMUX
B92-10	13123	B2-10-04	517-612	DEMUX
B92-10A	13124	B2-10A-01	269-442	DEMUX
B92-10A	13125	B2-10A-02	442-612	DEMUX
B92-10A	13126	B2-10A-03	612-786	DEMUX
B92-10A	13127	B2-10A-04	786-956	DEMUX
B92-10A	13128	B2-10A-05	956-1082	DEMUX
B92-11	13129	B2-11-01	1-160	DEMUX
B92-11	13130	B2-11-02	160-313	DEMUX
B92-11	13131	B2-11-03	313-472	DEMUX
B92-11	13132	B2-11-04	472-630	DEMUX
B92-11	13133	B2-11-05	630-785	DEMUX
B92-11	13134	B2-11-06	786-944	DEMUX
B92-11	13135	B2-11-07	944-1102	DEMUX
B92-11	13136	B2-11-08	1102-1258	DEMUX
B92-11	13137	B2-11-09	1258-1416	DEMUX
B92-11	13138	B2-11-10	1416-1571	DEMUX
B92-11	13139	B2-11-11	1571-1730	DEMUX
B92-11	13140	B2-11-12	1730-1889	DEMUX
B92-11	13141	B2-11-13	1889-2044	DEMUX
B92-11	13142	B2-11-14	2044-2137	DEMUX
B92-12	13143	B2-12-01	1-171	DEMUX
B92-12	13144	B2-12-02	171-346	DEMUX
B92-12	13145	B2-12-03	346-389	DEMUX
B92-13	13146	B2-13-01	1-159	DEMUX
B92-13	13147	B2-13-02	159-314	DEMUX
B92-13	13148	B2-13-03	314-473	DEMUX
B92-13	13149	B2-13-04	473-632	DEMUX
B92-13	13350	B2-13-05	632-791	DEMUX
B92-13	13351	B2-13-06	791-950	DEMUX
B92-13	13352	B2-13-07	950-1108	DEMUX
B92-13	13353	B2-13-08	1108-1266	DEMUX
B92-13	13354	B2-13-09	1266-1424	DEMUX
B92-13	13355	B2-13-10	1424-1583	DEMUX
B92-13	13356	B2-13-11	1583-1742	DEMUX
B92-13	13357	B2-13-12	1742-1900	DEMUX
B92-13	13358	B2-13-13	1900-2059	DEMUX
B92-13	13359	B2-13-14	2059-2217	DEMUX
B92-13	13360	B2-13-15	2217-2380	DEMUX
B92-13	13361	B2-13-16	2380-2539	DEMUX
B92-13	13362	B2-13-17	2539-2589	DEMUX

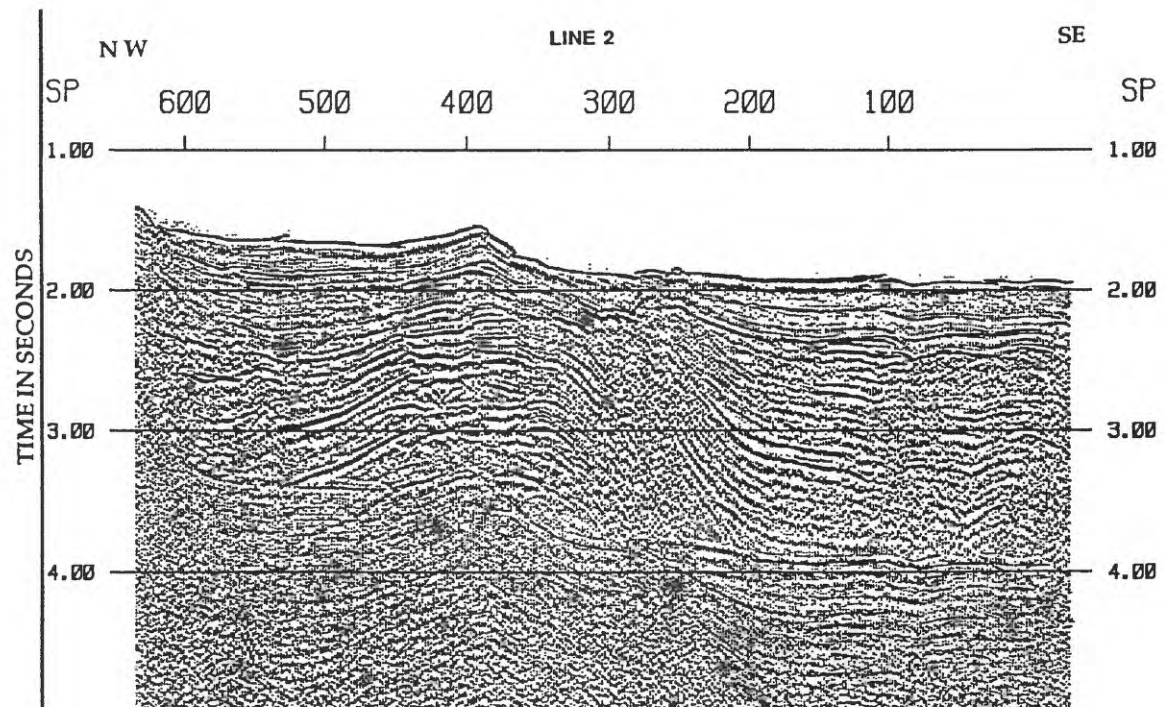
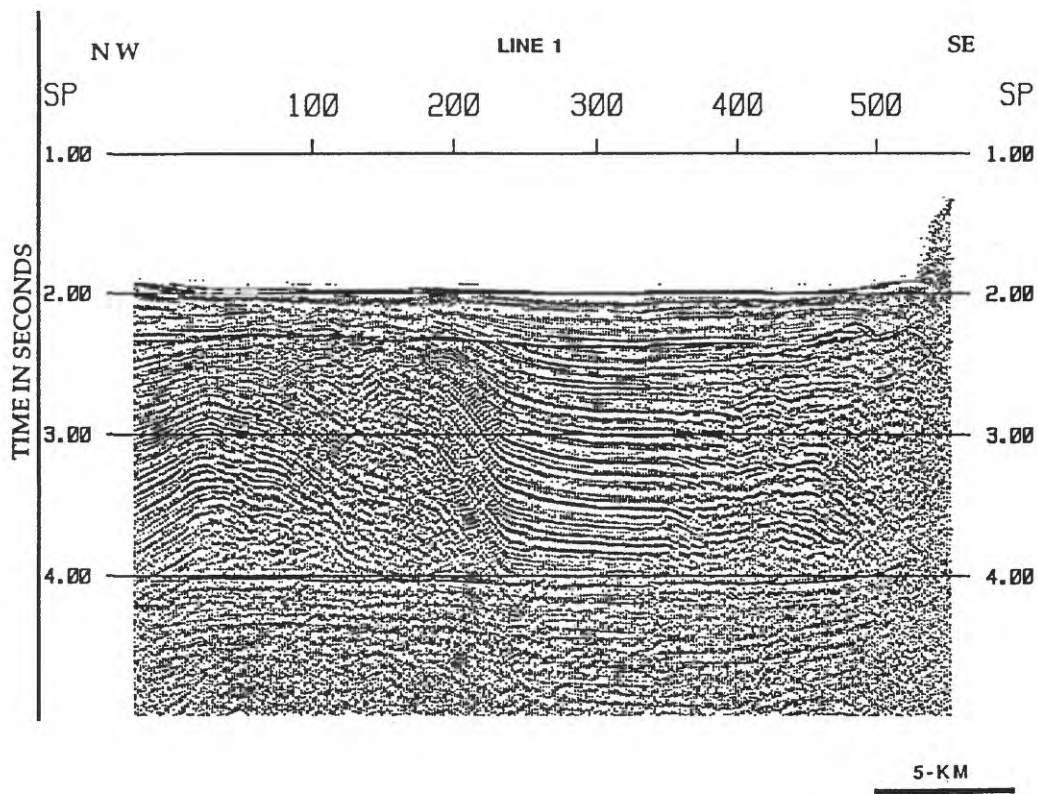
Line	Slot	Reel	File	Type
B92-14	13363	B2-14-01	1-174	DEMUX
B92-14	13364	B2-14-02	174-318	DEMUX
B92-14	13365	B2-14-03	318-445	DEMUX
B92-15	13366	B2-15-01	1-168	DEMUX
B92-15	13367	B2-15-02	168-327	DEMUX
B92-15	13368	B2-15-03	327-487	DEMUX
B92-15	13391	B2-15-04	487-645	DEMUX
B92-15	13392	B2-15-05	645-804	DEMUX
B92-15	13393	B2-15-06	804-962	DEMUX
B92-15	13394	B2-15-07	962-1120	DEMUX
B92-15	13395	B2-15-08	1120-1278	DEMUX
B92-15	13396	B2-15-09	1278-1436	DEMUX
B92-15	13397	B2-15-10	1436-1593	DEMUX
B92-15	13398	B2-15-11	1593-1750	DEMUX
B92-15	13399	B2-15-12	1750-1847	DEMUX
B92-15	13400	B2-15-13	1847-2006	DEMUX
B92-15	13401	B2-15-14	2006-2055	DEMUX
B92-16	13402	B2-16-01	1-324	DEMUX
B92-16	13403	B2-16-02	324-375	DEMUX
B92-17	13404	B2-17-01	4-165	DEMUX
B92-17	13405	B2-17-02	165-319	DEMUX
B92-17	13406	B2-17-03	319-477	DEMUX
B92-17	13407	B2-17-04	477-634	DEMUX
B92-17	13408	B2-17-05	634-792	DEMUX
B92-17	13409	B2-17-06	792-950	DEMUX
B92-17	13410	B2-17-07	950-1108	DEMUX
B92-17	13411	B2-17-08	1108-1266	DEMUX
B92-17	13412	B2-17-09	1266-1425	DEMUX
B92-17	13413	B2-17-10	1425-1579	DEMUX
B92-17	13414	B2-17-11	1579-1738	DEMUX
B92-17	13415	B2-17-12	1738-1895	DEMUX
B92-17	13416	B2-17-13	1895-2052	DEMUX
B92-17	13417	B2-17-14	2052-2210	DEMUX
B92-17	13418	B2-17-15	2210-2368	DEMUX
B92-17	13419	B2-17-16	2368-2526	DEMUX
B92-17	13420	B2-17-17	2526-2680	DEMUX
B92-17	13421	B2-17-18	2680-2683	DEMUX
B92-17	13422	B2-17-19	2758-2904	DEMUX
B92-17	13423	B2-17-20	2904-3059	DEMUX
B92-17	13424	B2-17-21	3059-3217	DEMUX
B92-17	13694	B2-17-22	3217-3269	DEMUX
B92-17OB	13695	B217B-01	1-97	DEMUX
B92-17OB	13696	B217B-02	97-195	DEMUX
B92-17OB	13697	B217B-03	195-289	DEMUX
B92-17OB	13698	B217B-04	289-387	DEMUX
B92-17OB	13699	B217B-05	387-485	DEMUX
B92-17OB	13700	B217B-06	485-582	DEMUX
B92-17OB	13701	B217B-07	582-641	DEMUX

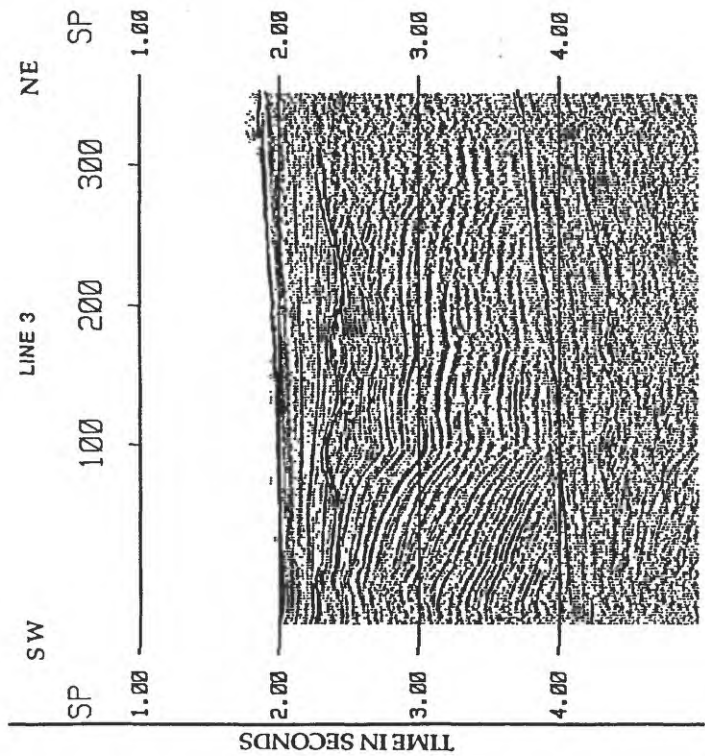
Line	Slot	Reel	File	Type
B92-18	13702	B2-18-01	1-326	DEMUX
B92-18	13703	B2-18-02	326-419	DEMUX
B92-19	15056	B2-19-01	1-159	DEMUX
B92-19	15057	B2-19-02	159-316	DEMUX
B92-19	15058	B2-19-03	316-475	DEMUX
B92-19	15059	B2-19-04	475-614	DEMUX
B92-20	15060	B2-20-01	1-174	DEMUX
B92-20	15061	B2-20-02	174-344	DEMUX
B92-20	15062	B2-20-03	344-412	DEMUX
B92-21	15063	B2-21-01	1-155	DEMUX
B92-21	15064	B2-21-02	155-311	DEMUX
B92-21	15065	B2-21-03	311-465	DEMUX
B92-21	15066	B2-21-04	465-620	DEMUX
B92-21	15067	B2-21-05	620-774	DEMUX
B92-21	15068	B2-21-06	774-839	DEMUX
B92-22	15069	B2-22-01	7-180	DEMUX
B92-22	15070	B2-22-02	180-350	DEMUX
B92-22	15071	B2-22-03	350-447	DEMUX
B92-23	15072	B2-23-01	1-158	DEMUX
B92-23	15073	B2-23-02	158-214	DEMUX
B92-24	15074	B2-24-01	5-345	DEMUX
B92-24	15075	B2-24-02	345-468	DEMUX
B92-25	15076	B2-25-01	1-158	DEMUX
B92-25	15077	B2-25-02	158-313	DEMUX
B92-25	15078	B2-25-03	313-471	DEMUX
B92-25	15079	B2-25-04	471-627	DEMUX
B92-25	15080	B2-25-05	627-785	DEMUX
B92-25	15081	B2-25-06	785-940	DEMUX
B92-25	15082	B2-25-07	940-1098	DEMUX
B92-25	15083	B2-25-08	1098-1253	DEMUX
B92-25	15084	B2-25-09	1253-1411	DEMUX
B92-25	15085	B2-25-10	1411-1513	DEMUX
B92-26	15086	B2-26-01	1-171	DEMUX
B92-26	15087	B2-26-02	171-344	DEMUX
B92-26	15088	B2-26-03	344-514	DEMUX
B92-26	15089	B2-26-04	515-682	DEMUX
B92-28	15090	B2-28-01	1-175	DEMUX
B92-28	15091	B2-28-02	175-348	DEMUX
B92-28	15092	B2-28-03	348-422	DEMUX
B92-30	15093	B2-30-01	2-174	DEMUX
B92-32	15094	B2-32-01	1-158	DEMUX
B92-32	15095	B2-32-02	158-313	DEMUX
B92-32	15096	B2-32-03	313-472	DEMUX
B92-32	15377	B2-32-04	472-515	DEMUX
B92-34	15378	B2-34-01	1-156	DEMUX
B92-34	15379	B2-34-02	156-314	DEMUX
B92-34	15380	B2-34-03	314-469	DEMUX
B92-34	15381	B2-34-04	469-627	DEMUX

Line	Slot	Reel	File	Type
B92-34	15382	B2-34-05	627-682	DEMUX
B92-36	15383	B2-36-01	1-158	DEMUX
B92-36	15384	B2-36-02	158-316	DEMUX
B92-36	15385	B2-36-03	316-474	DEMUX
B92-36	15540	B2-36-04	474-525	DEMUX
B92-38	15541	B2-38-01	3-161	DEMUX
B92-38	15542	B2-38-02	161-318	DEMUX
B92-38	15543	B2-38-03	318-480	DEMUX
B92-38	15544	B2-38-04	480-638	DEMUX
B92-38	15545	B2-38-05	638-727	DEMUX
B92-40	15546	B2-40-01	2-162	DEMUX
B92-40	15547	B2-40-02	162-272	DEMUX
B92-40A	15548	B240A-03	241-400	DEMUX
B92-40A	15549	B240A-04	400-560	DEMUX
B92-40A	15550	B240A-05	560-716	DEMUX
B92-40A	15551	B240A-06	716-860	DEMUX
B92-42	15552	B2-42-01	1-161	DEMUX
B92-42	15553	B2-42-02	161-316	DEMUX
B92-42	15554	B2-42-03	316-470	DEMUX
B92-42	15555	B2-42-04	470-637	DEMUX
B92-42	15556	B2-42-05	637-792	DEMUX
B92-42	15557	B2-42-06	792-951	DEMUX
B92-42	15558	B2-42-07	951-1109	DEMUX
B92-42	15559	B2-42-08	1109-1270	DEMUX
B92-42	15560	B2-42-09	1270-1321	DEMUX
B92-44	3717	B2-44-01	1-157	DEMUX
B92-44	3718	B2-44-02	157-312	DEMUX
B92-44	3719	B2-44-03	312-468	DEMUX
B92-44	3720	B2-44-04	468-625	DEMUX
B92-44	3721	B2-44-05	625-780	DEMUX
B92-44	3722	B2-44-06	780-938	DEMUX
B92-44	3723	B2-44-07	938-1098	DEMUX
B92-44	3724	B2-44-08	1098-1202	DEMUX
B92-46	3725	B2-46-01	1-62	DEMUX
B92-46	3726	B2-46-02	62-220	DEMUX
B92-46	3737	B2-46-03	220-388	DEMUX
B92-46	3738	B2-46-04	388-549	DEMUX
B92-46	3739	B2-46-05	549-723	DEMUX
B92-46	3740	B2-46-06	723-888	DEMUX
B92-46	3741	B2-46-07	888-1050	DEMUX
B92-46	3742	B2-46-08	1050-1182	DEMUX
B92-48	3743	B2-48-01	2-162	DEMUX
B92-48	3744	B2-48-02	162-322	DEMUX
B92-48	3745	B2-48-03	322-480	DEMUX
B92-48	3746	B2-48-04	480-636	DEMUX
B92-48	3747	B2-48-05	636-792	DEMUX
B92-48	3748	B2-48-06	792-950	DEMUX
B92-48	3749	B2-48-07	950-1110	DEMUX

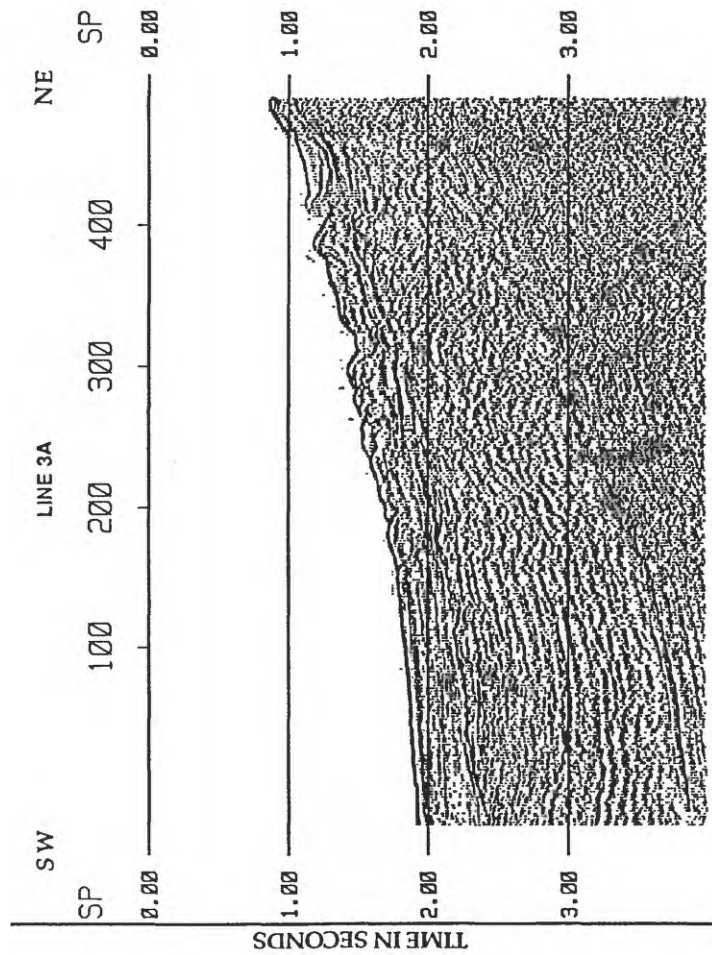
Line	Slot	Reel	File	Type
B92-50	3750	B2-50-01	1-176	DEMUX
B92-50	3751	B2-50-02	176-335	DEMUX
B92-50	3752	B2-50-03	335-492	DEMUX
B92-50	3753	B2-50-04	492-648	DEMUX
B92-50	3754	B2-50-05	648-680	DEMUX
B92-50A	3755	B250A-01	1-148	DEMUX
B92-50B	3756	B250B-01	2-165	DEMUX
B92-50B	3757	B250B-02	165-331	DEMUX
B92-50B	3758	B250B-03	331-489	DEMUX
B92-50B	3759	B250B-04	489-635	DEMUX
B92-52	3760	B2-52-01	1-155	DEMUX
B92-52	3761	B2-52-02	155-310	DEMUX
B92-52	3762	B2-52-03	310-467	DEMUX
B92-52	3763	B2-52-04	467-495	DEMUX
B92-54	3764	B2-54-01	1-190	DEMUX
B92-54	3765	B2-54-02	190-380	DEMUX
B92-54	3766	B2-54-03	380-569	DEMUX
B92-54	3777	B2-54-04	569-762	DEMUX
B92-54	3778	B2-54-05	762-780	DEMUX
B92-56	3779	B2-56-01	1-193	DEMUX
B92-56	3780	B2-56-02	193-383	DEMUX
B92-56	3781	B2-56-03	383-576	DEMUX
B92-56	3782	B2-56-04	576-765	DEMUX
B92-56	3783	B2-56-05	765-958	DEMUX
B92-56	3784	B2-56-06	958-1143	DEMUX
B92-58	3785	B2-58-01	1-192	DEMUX
B92-58	3786	B2-58-02	192-381	DEMUX
B92-58	3787	B2-58-03	381-573	DEMUX
B92-58	3788	B2-58-04	573-766	DEMUX
B92-58	3789	B2-58-05	766-958	DEMUX
B92-58	3790	B2-58-06	958-1138	DEMUX
B92-60	3791	B2-60-01	1-190	DEMUX
B92-60	3792	B2-60-02	190-378	DEMUX
B92-60	3793	B2-60-03	378-543	DEMUX

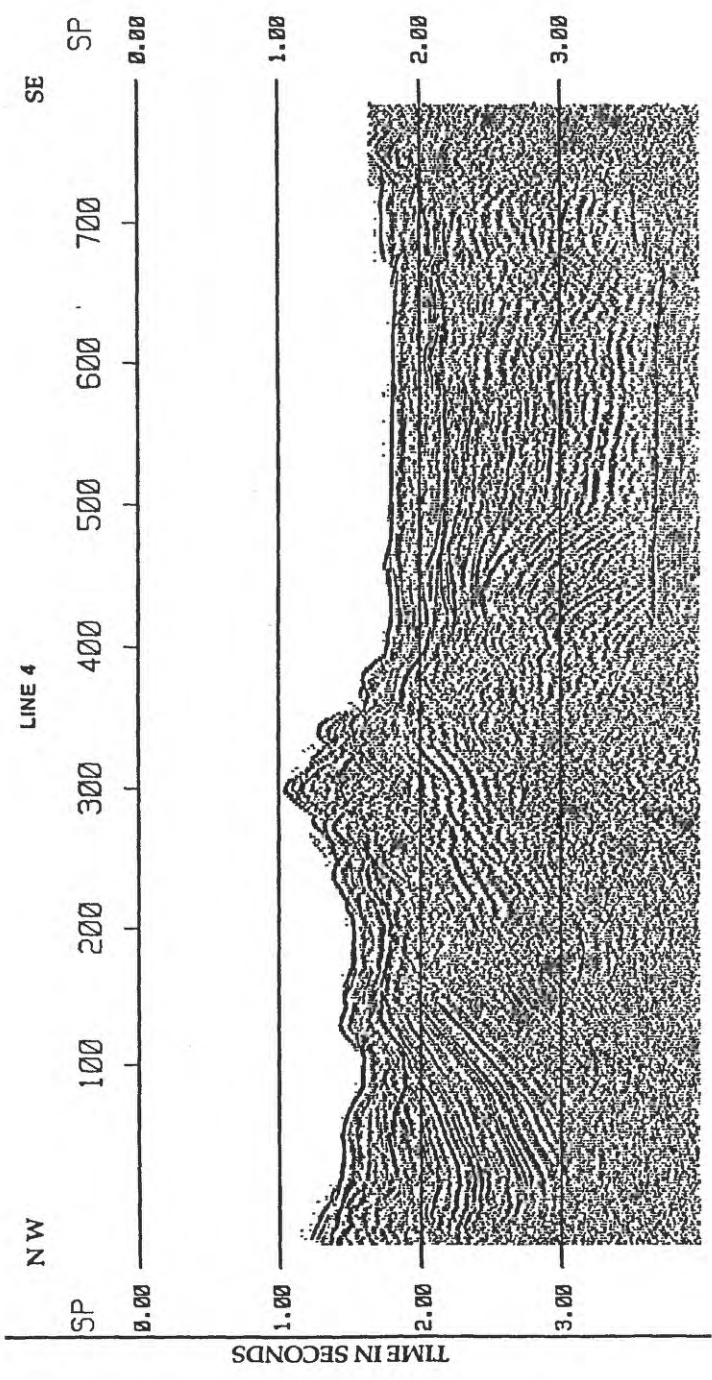
# APPENDIX B - PROFILES



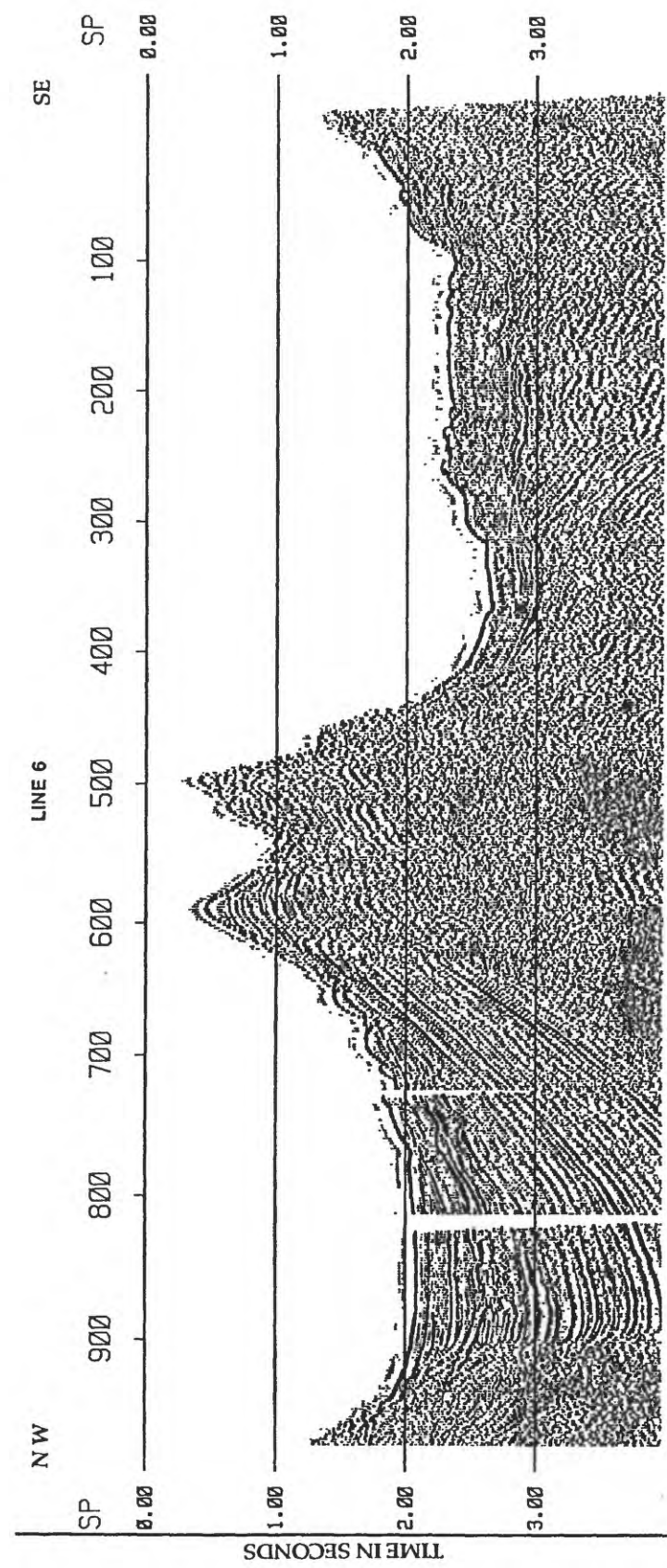


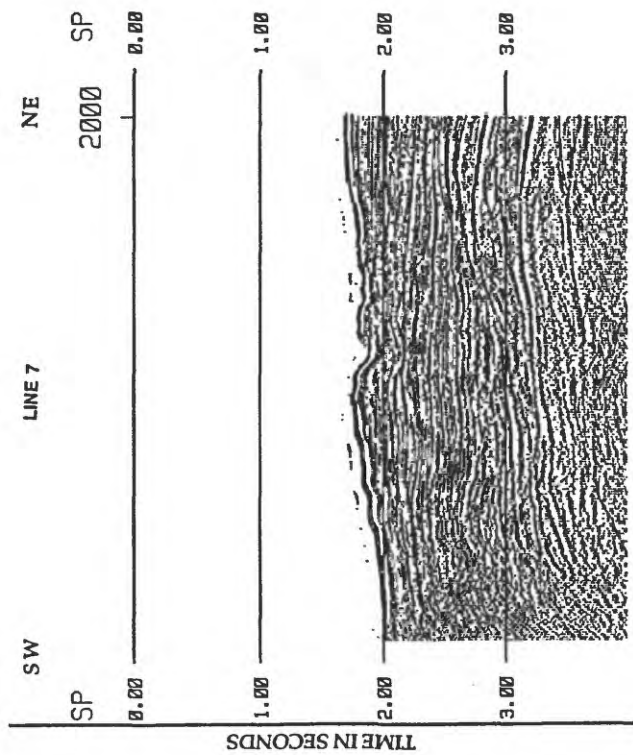
5-KM



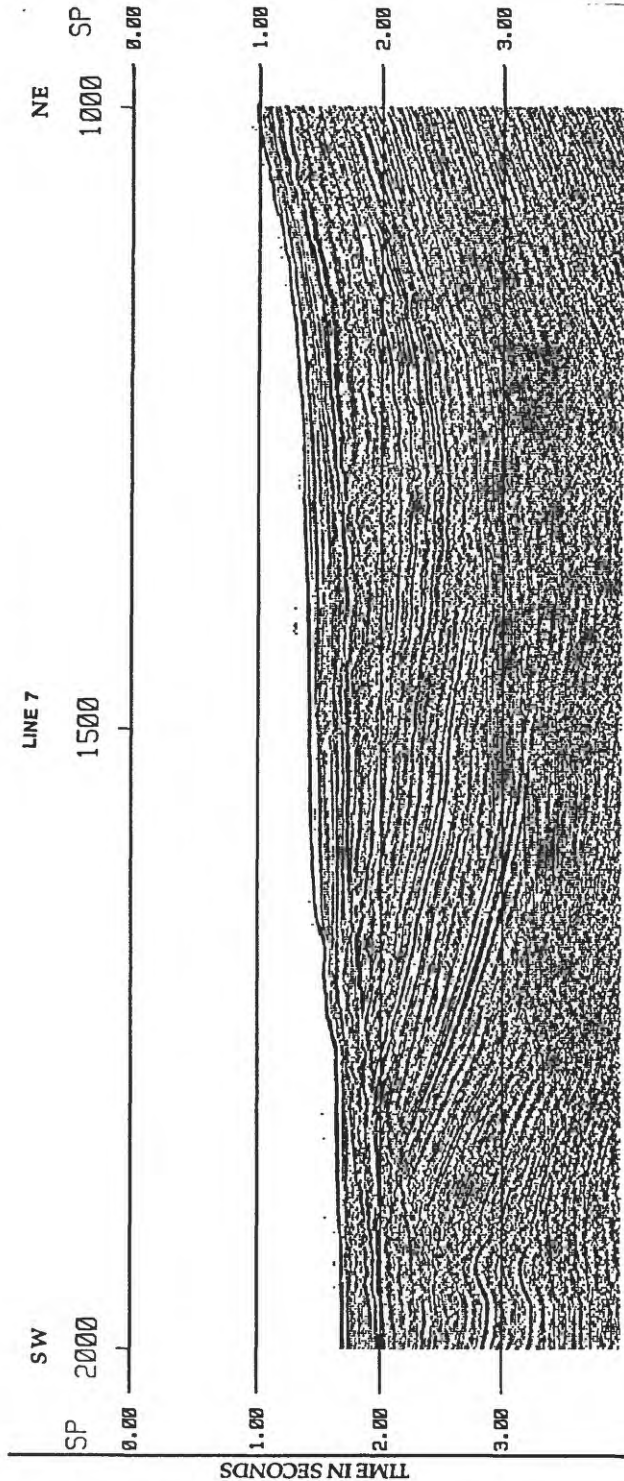


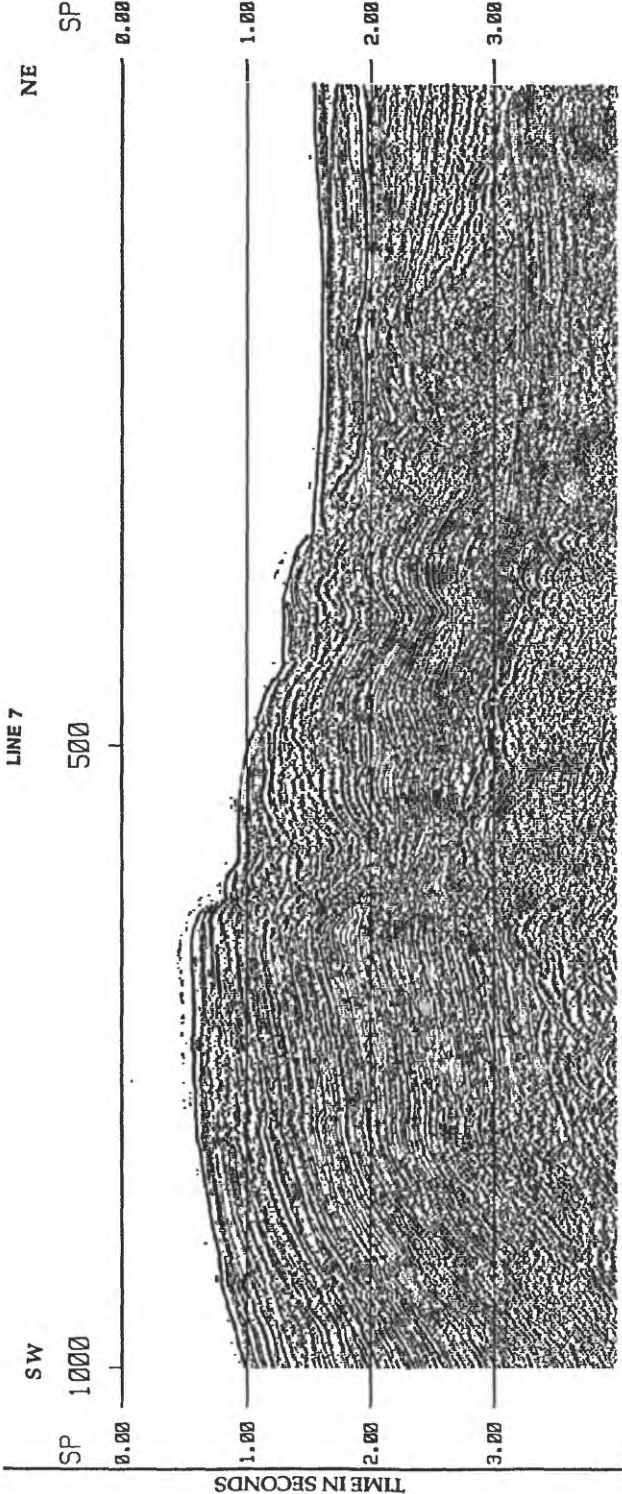
5-KM



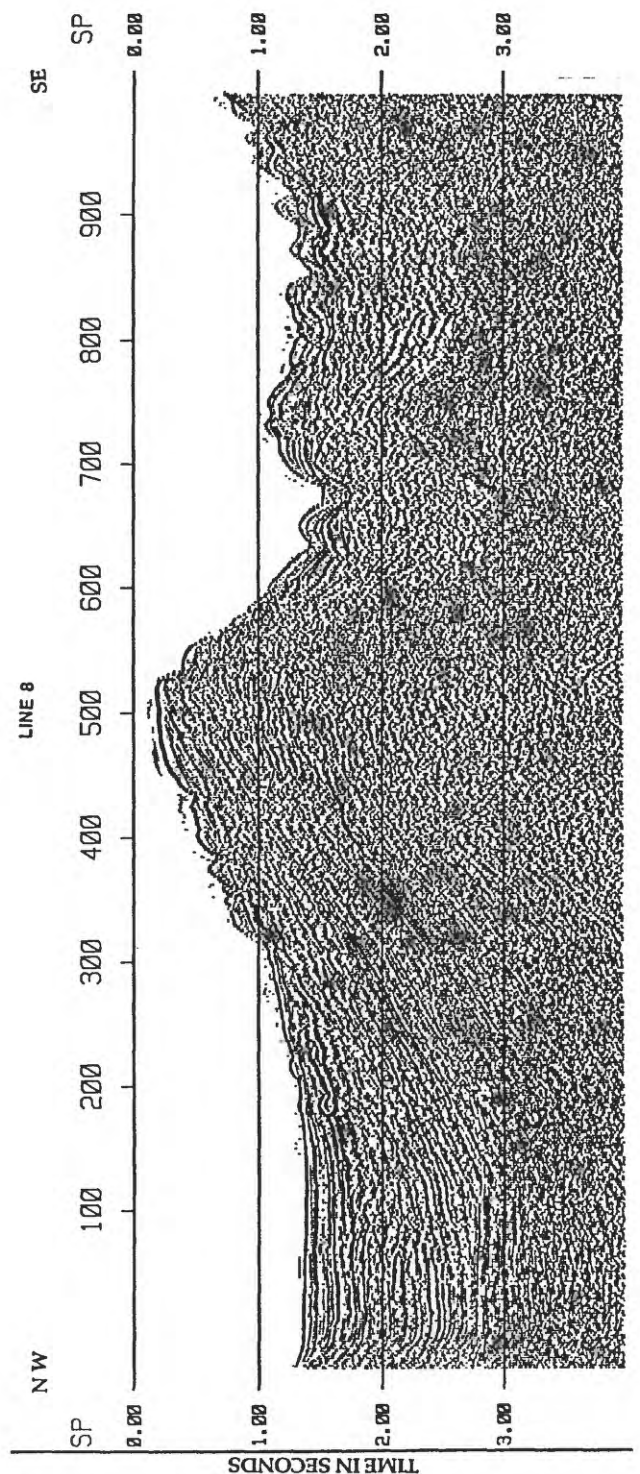


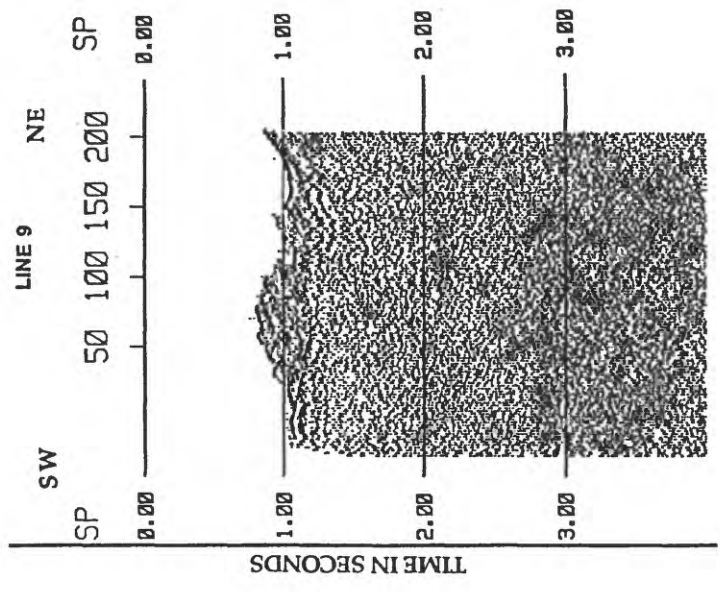
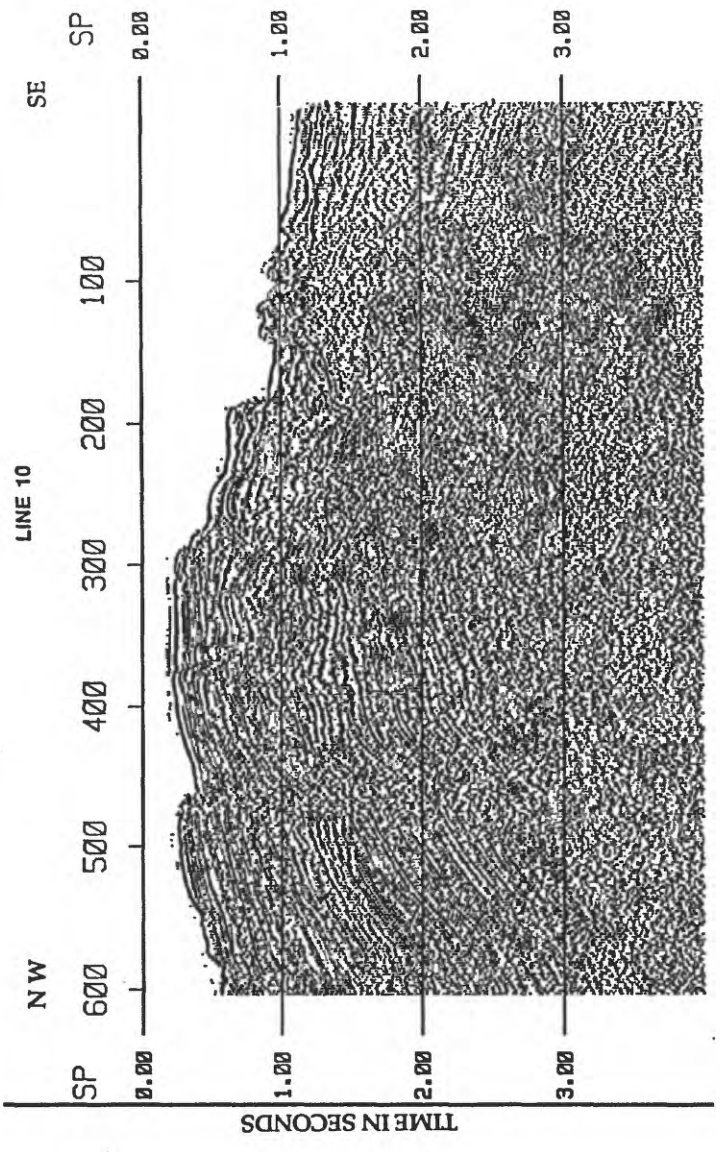
5-KM



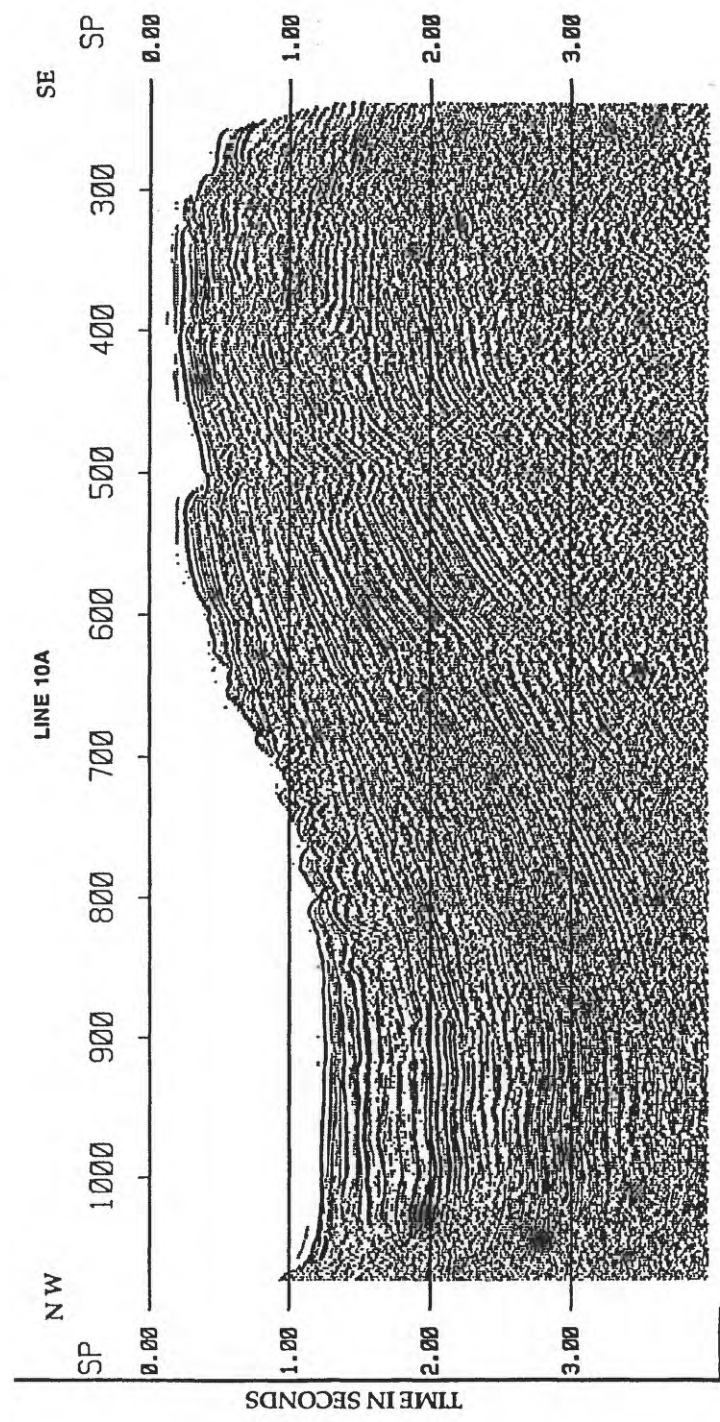


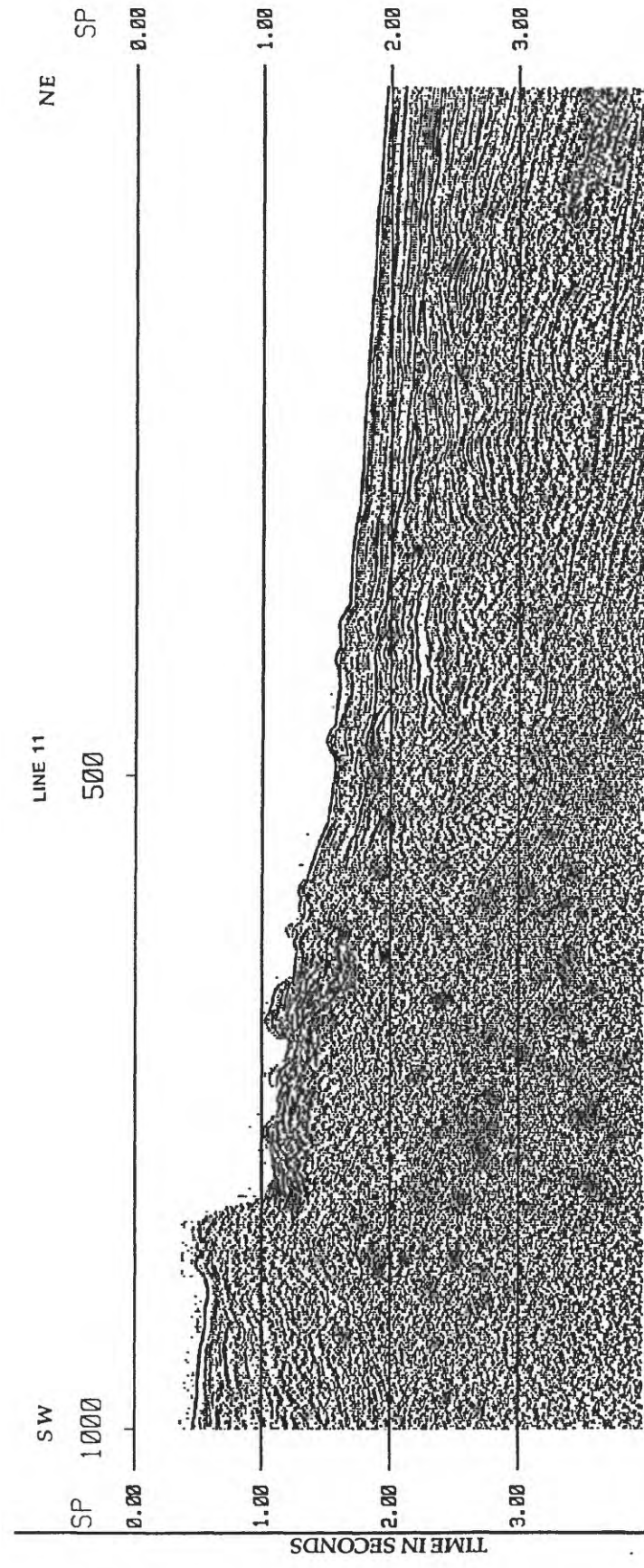
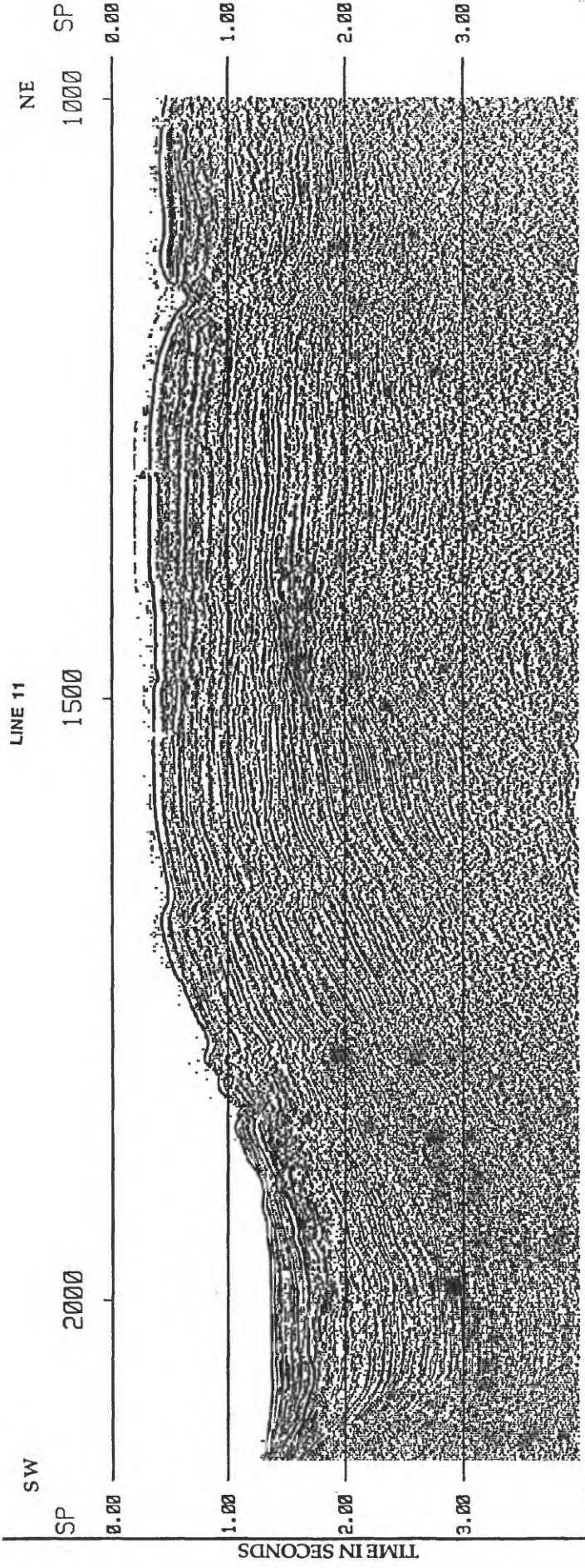
5 KM

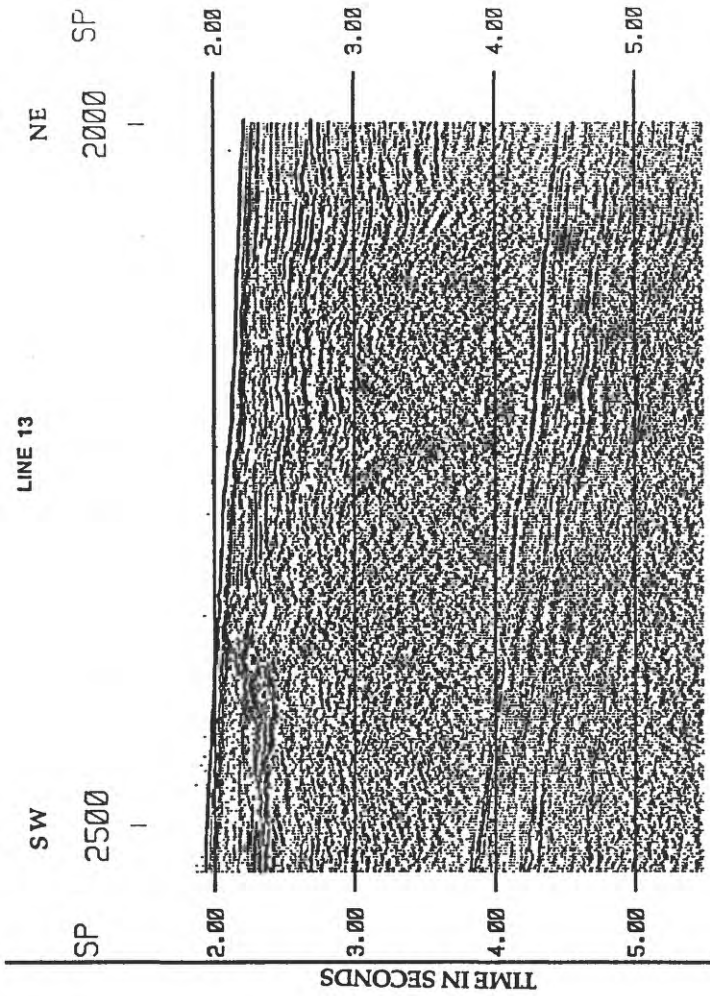




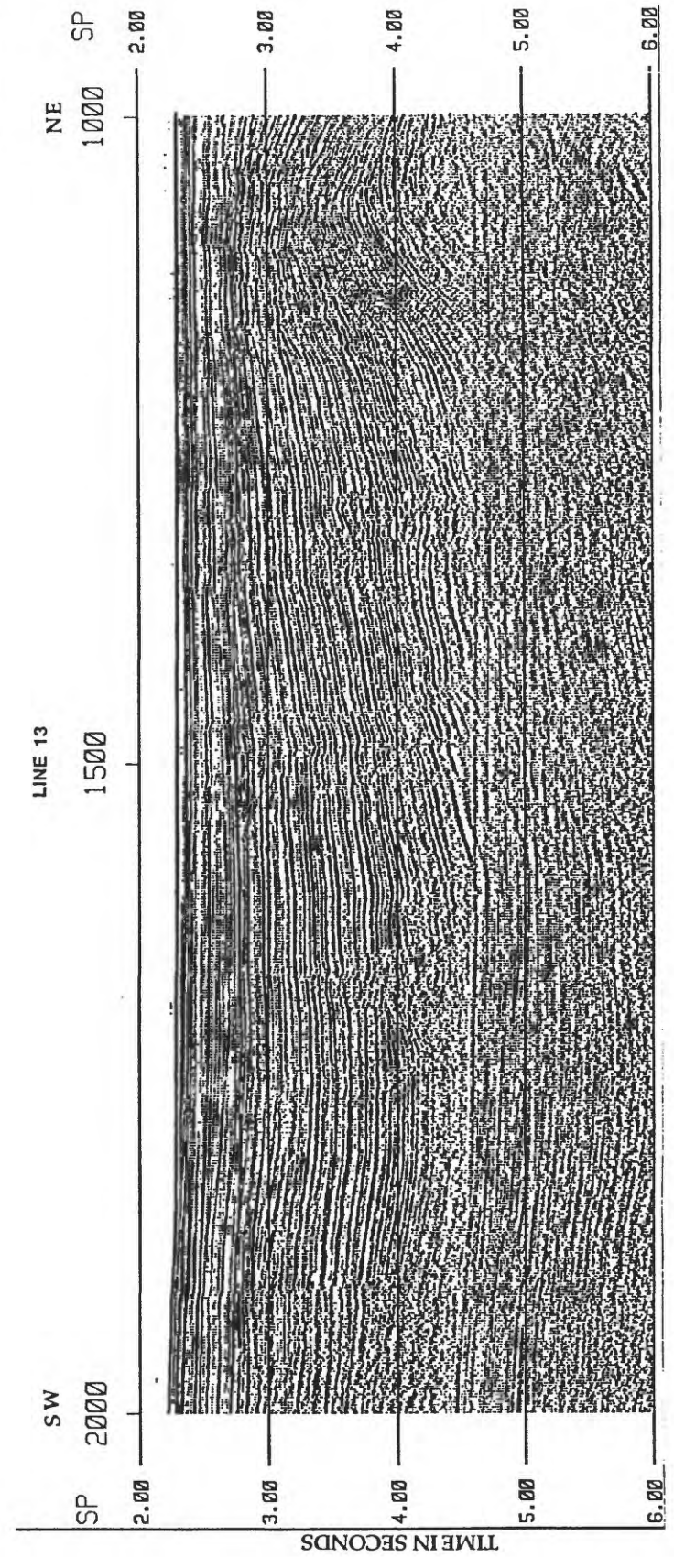
5-KM

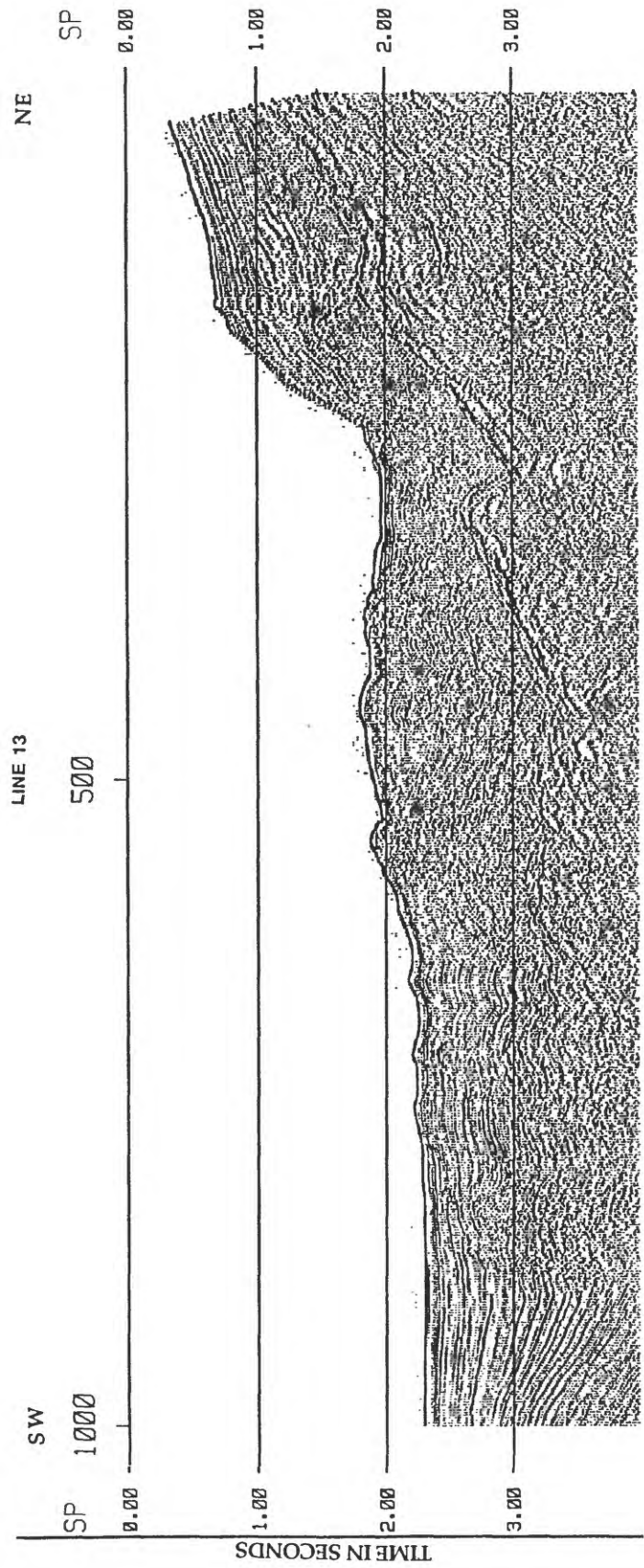




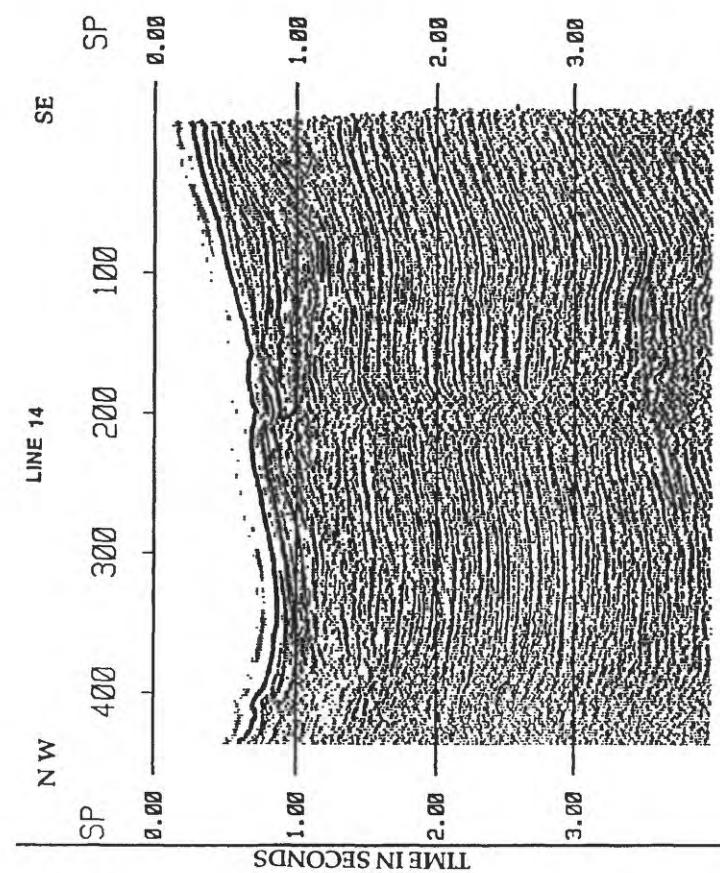
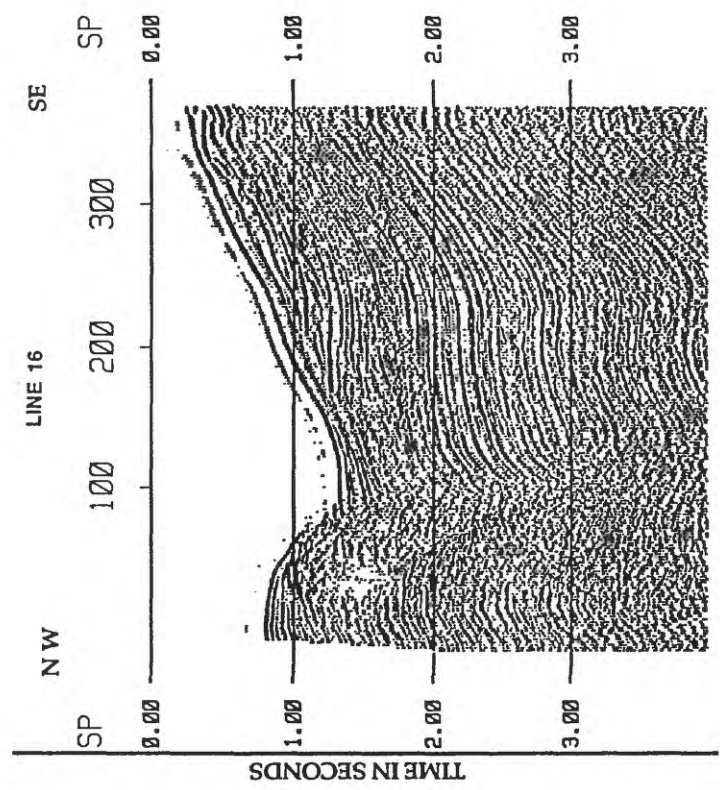


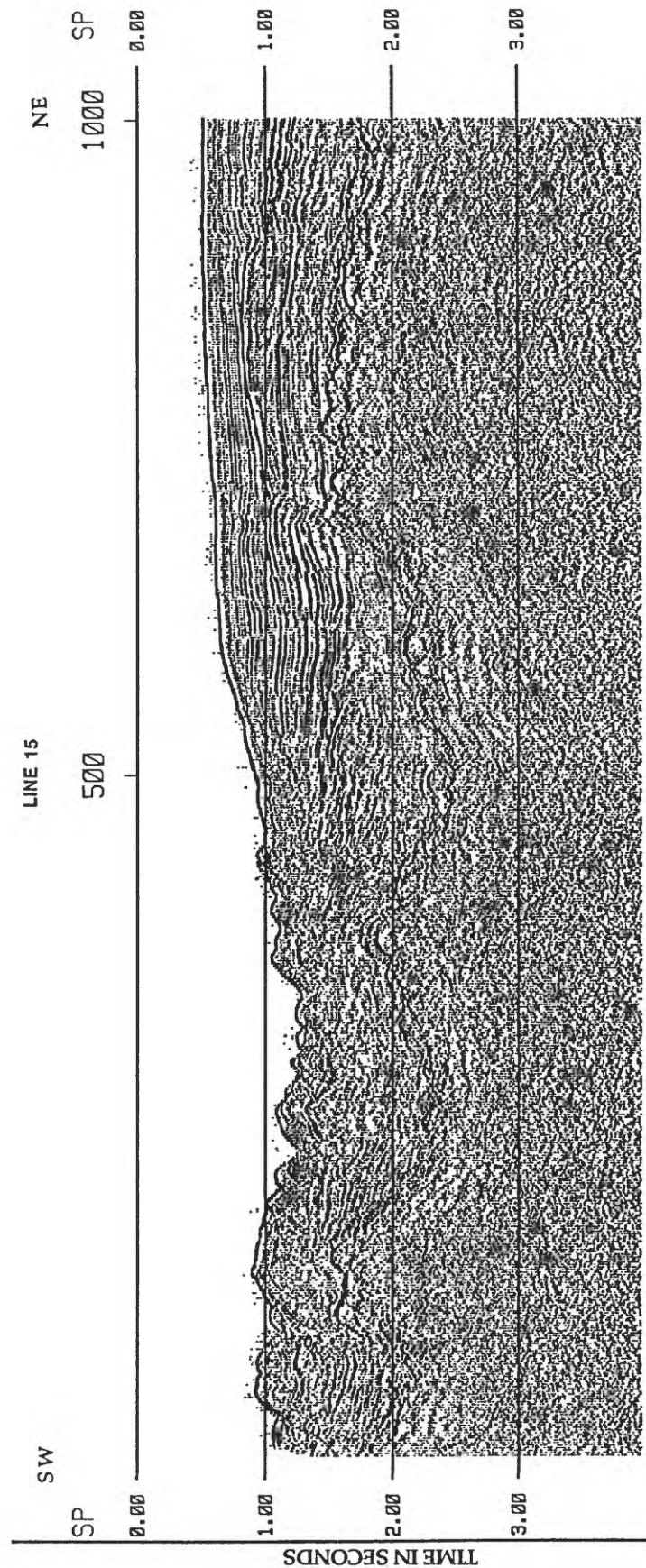
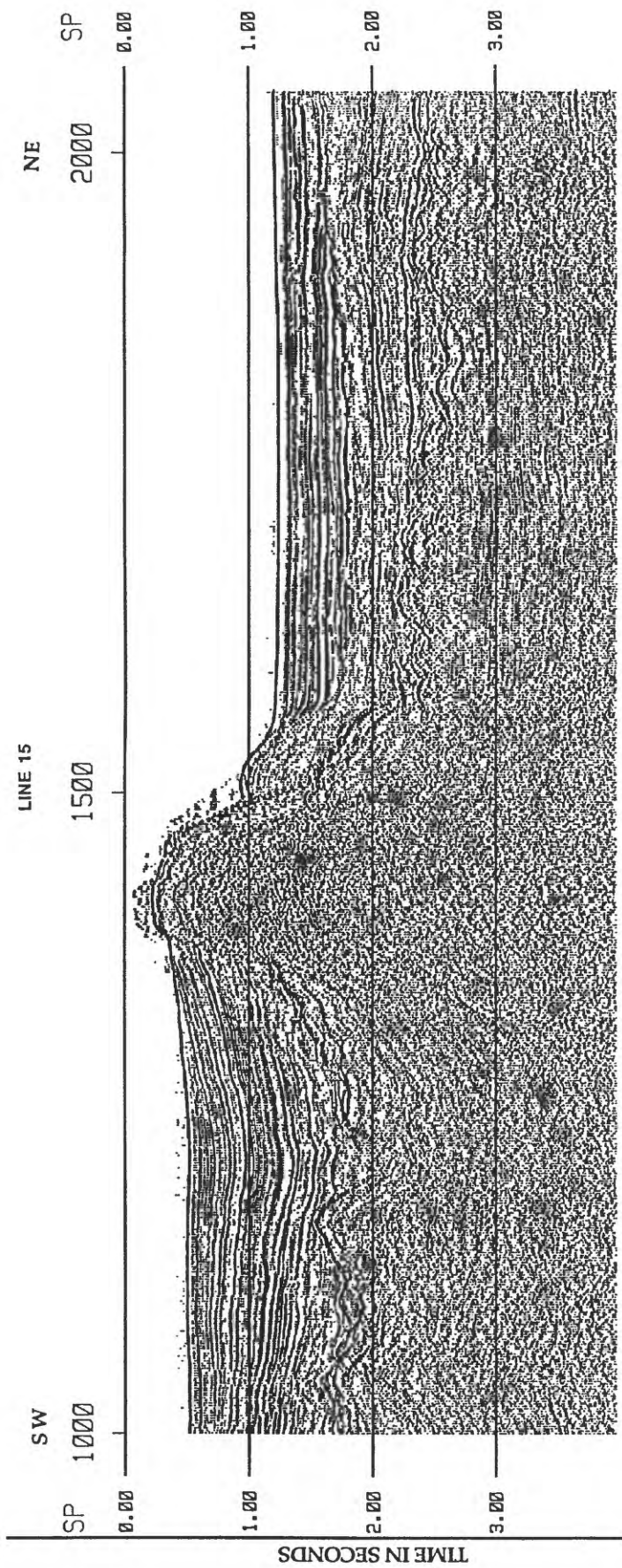
5-KM

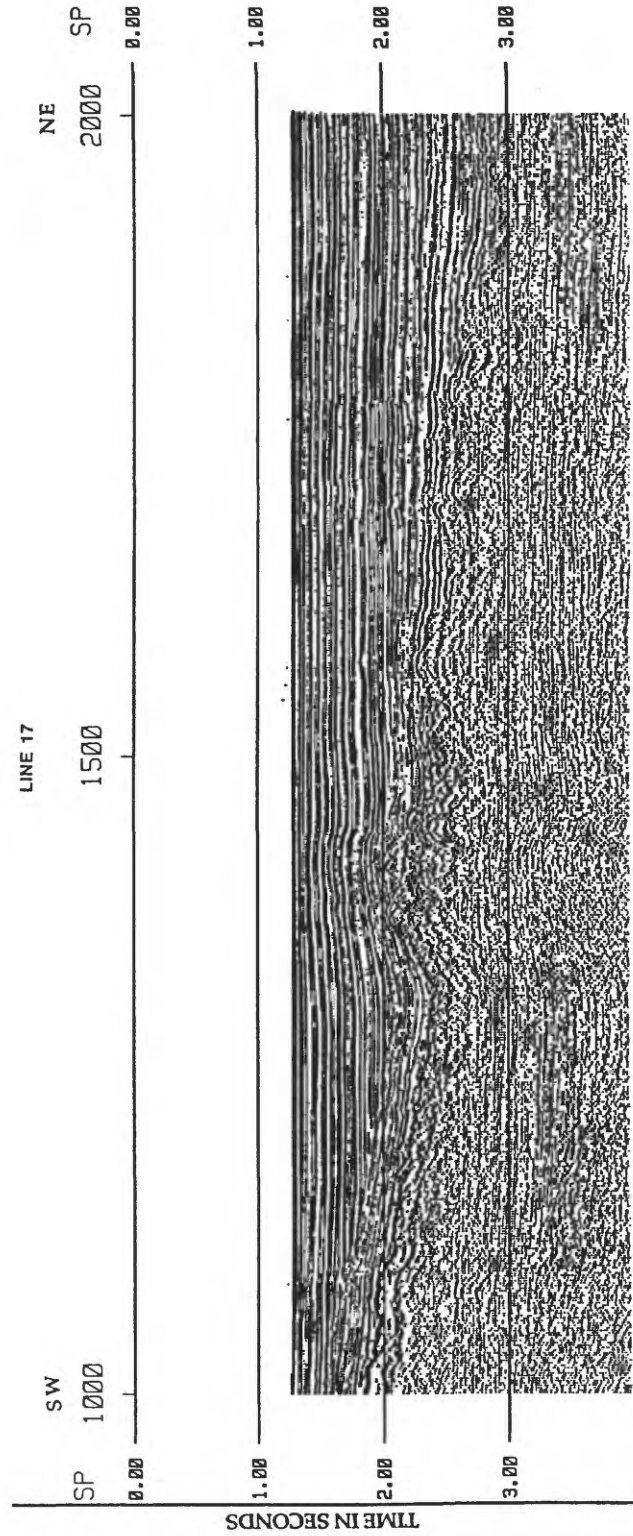
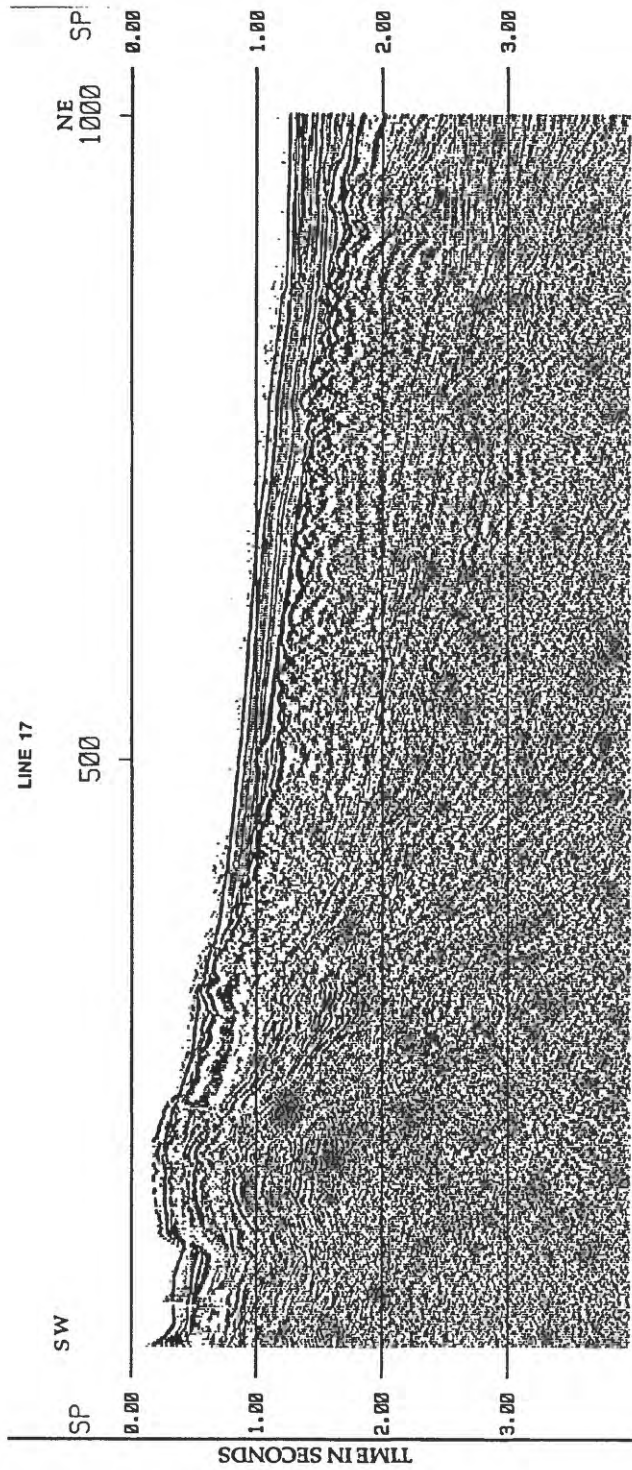


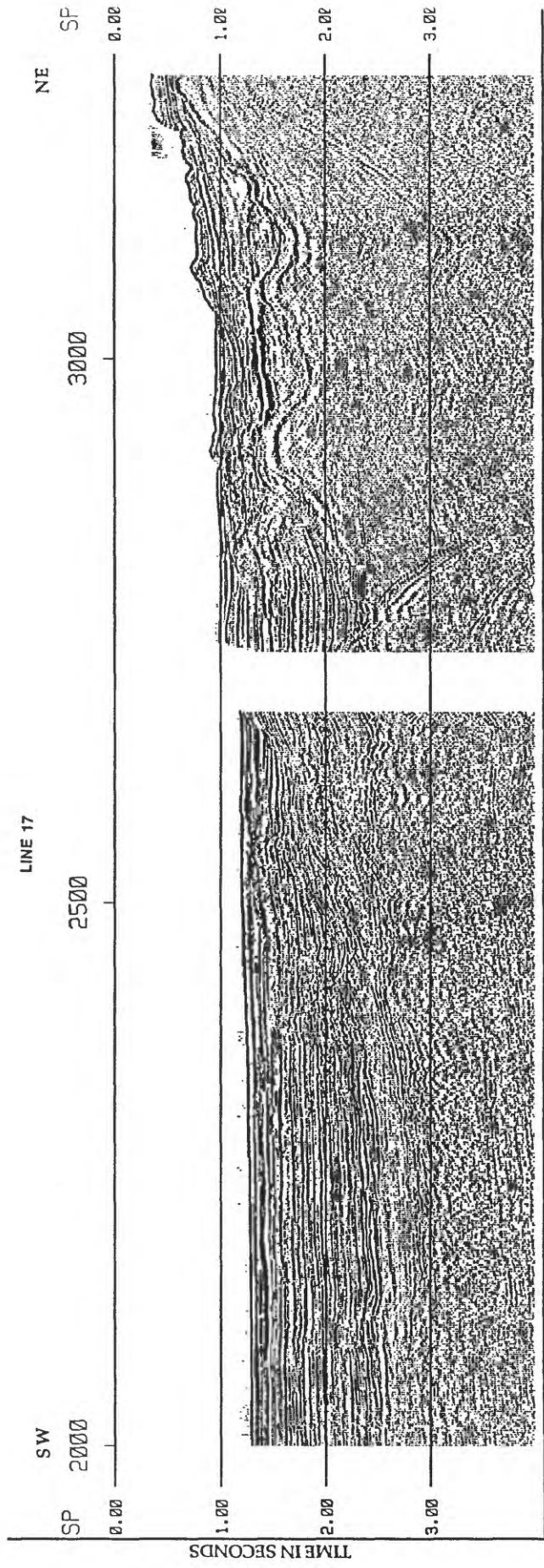


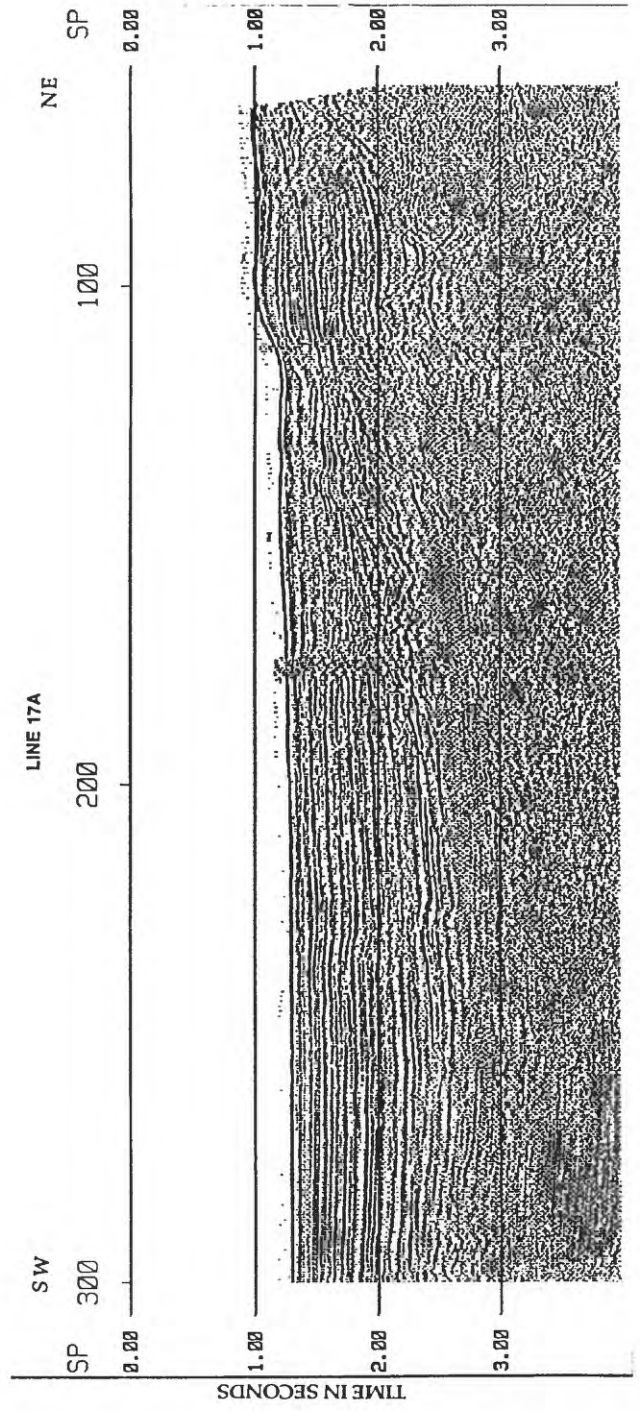
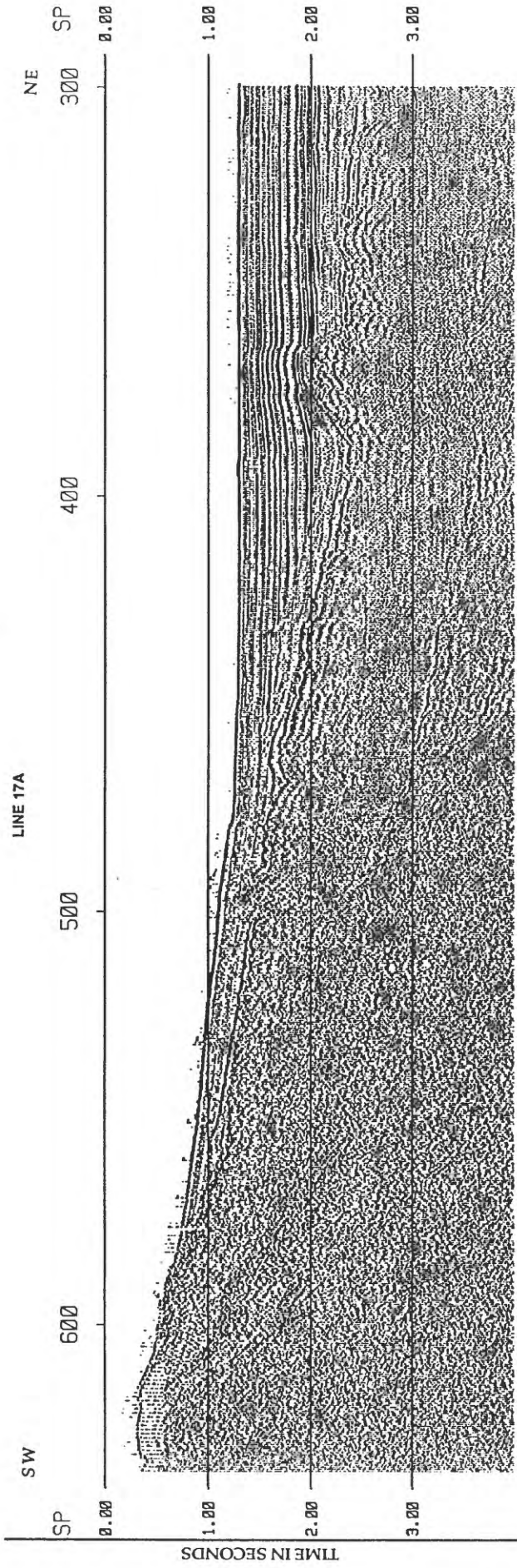
5-KM

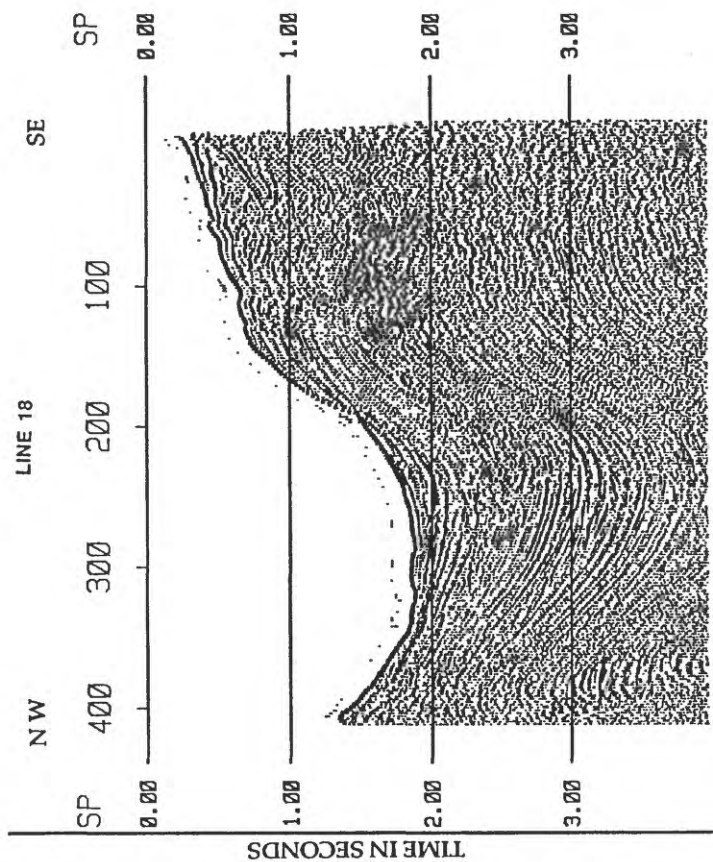




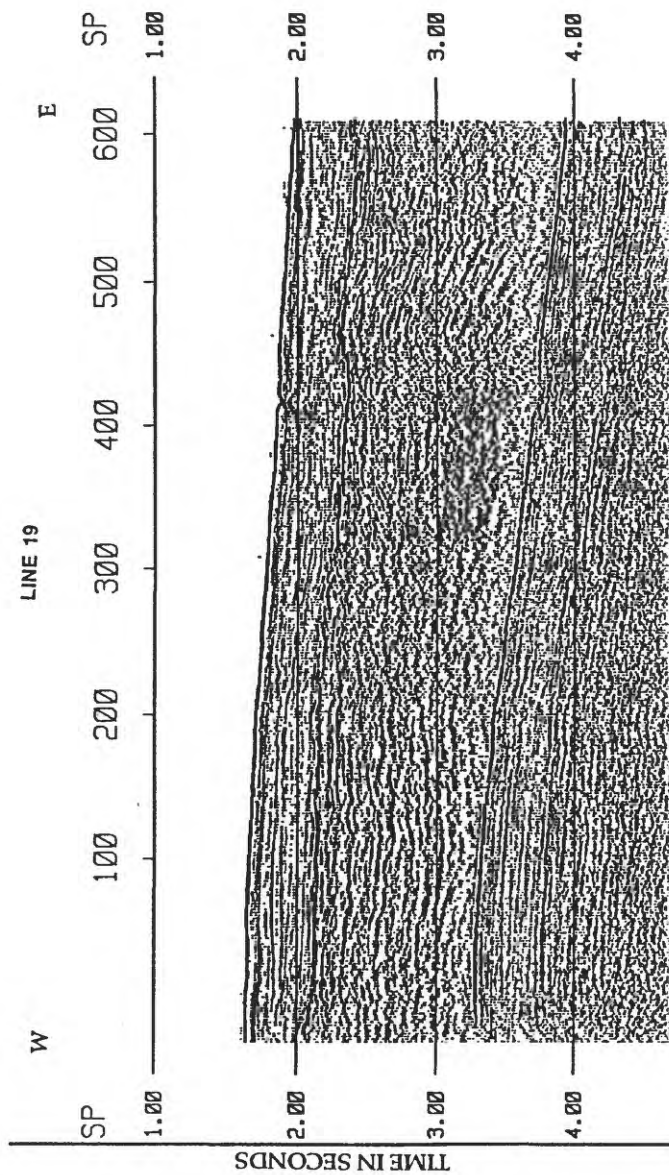


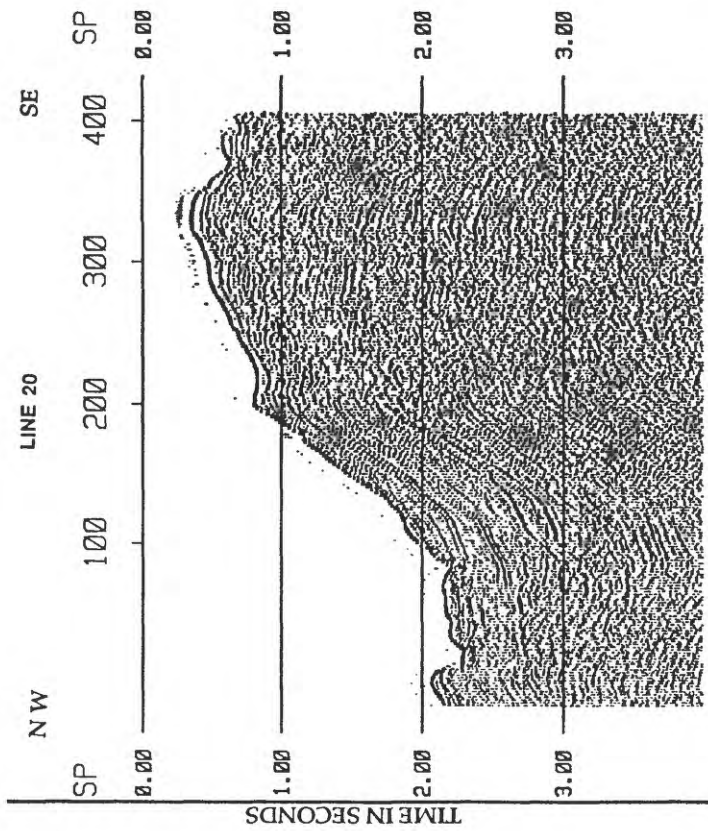




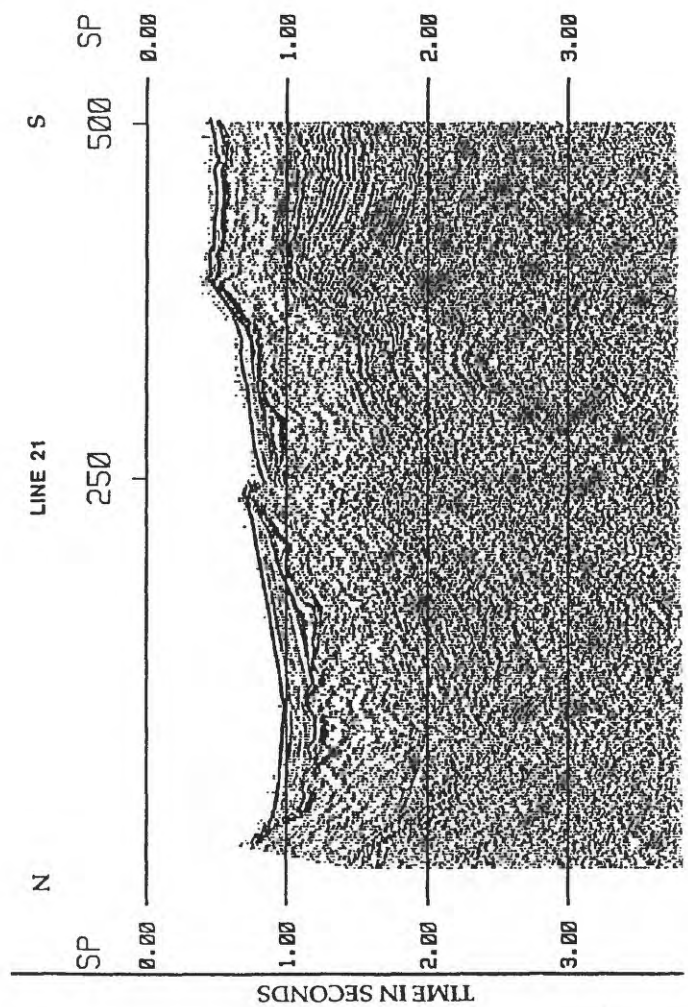


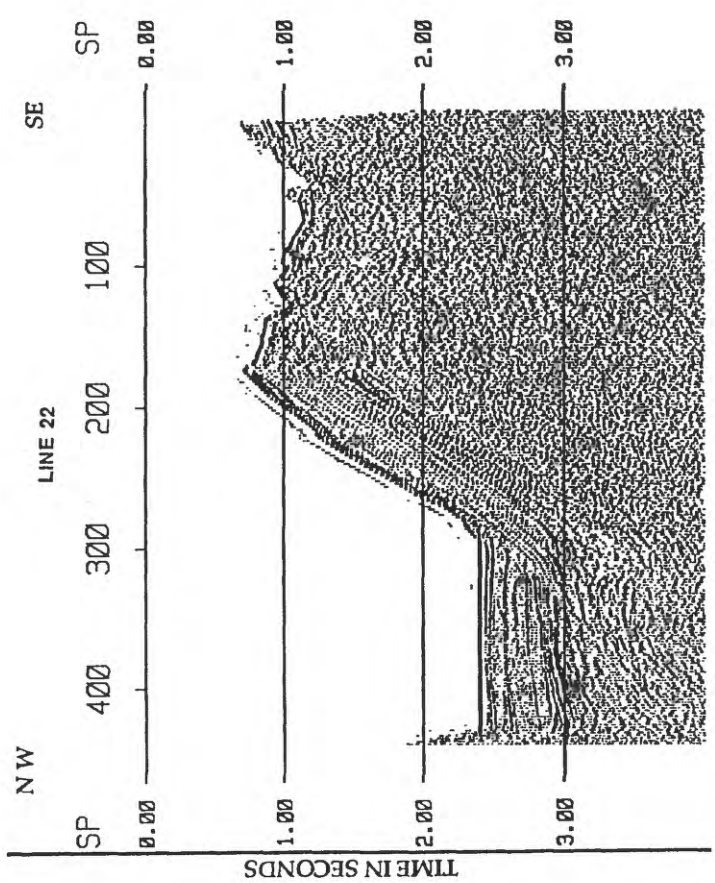
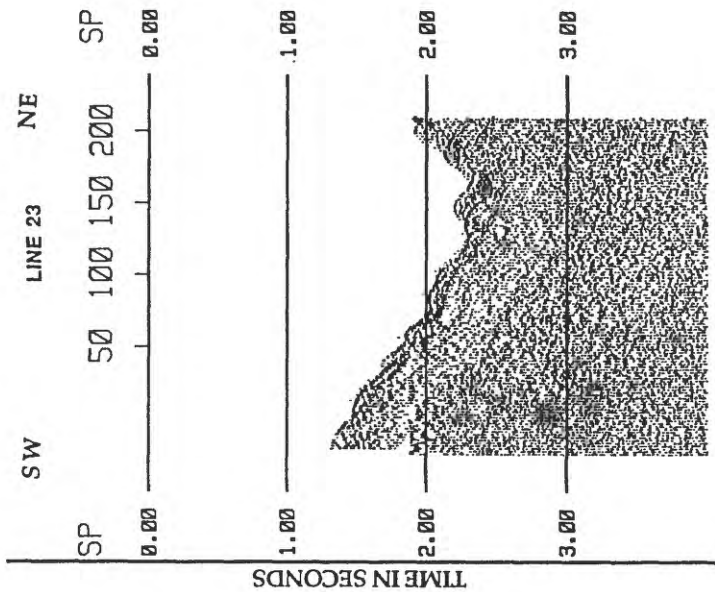
5-KM



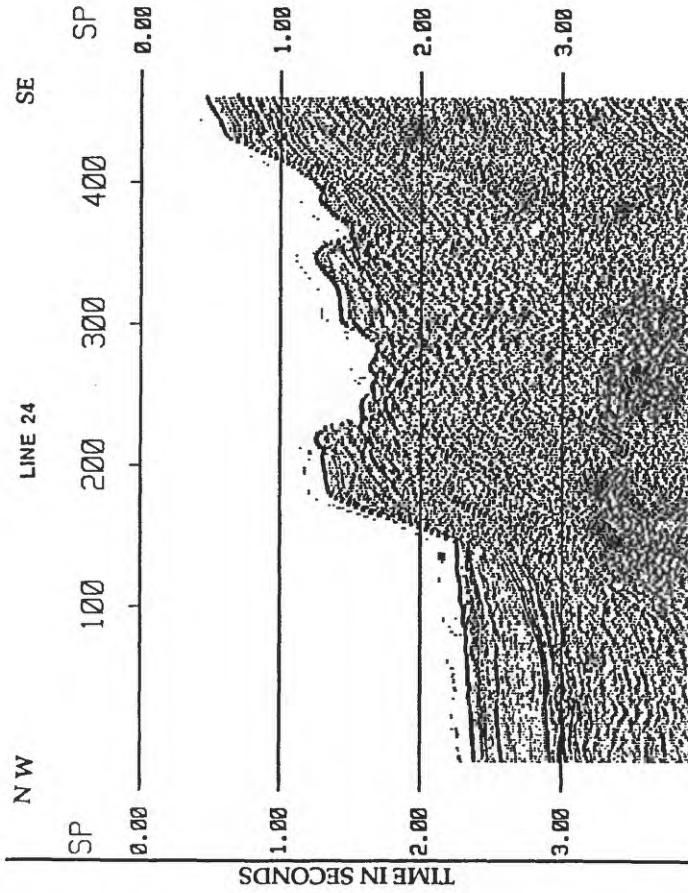


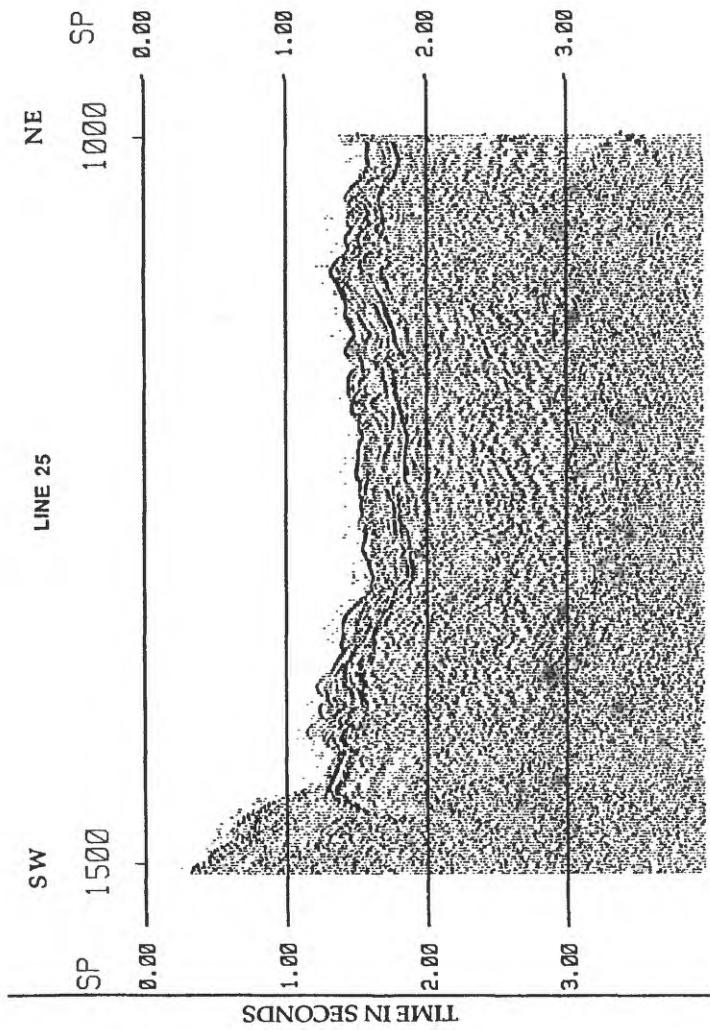
5-KM



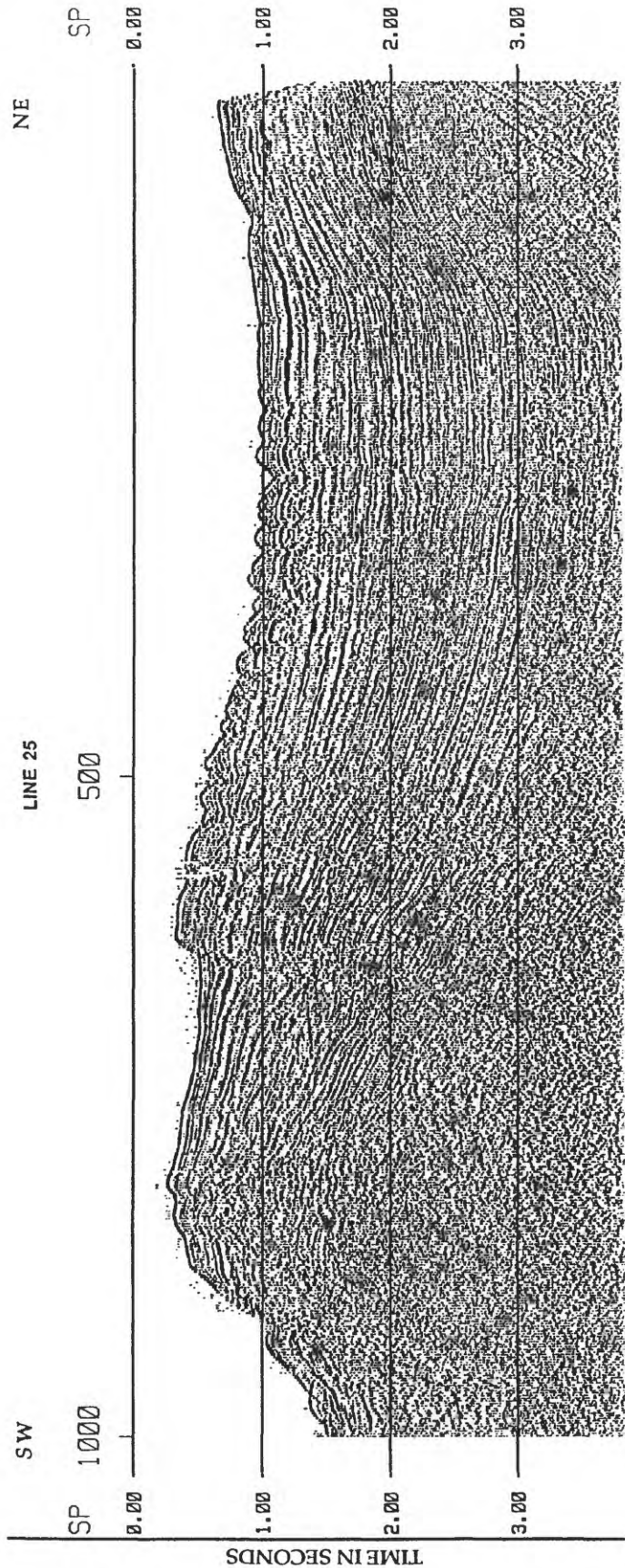


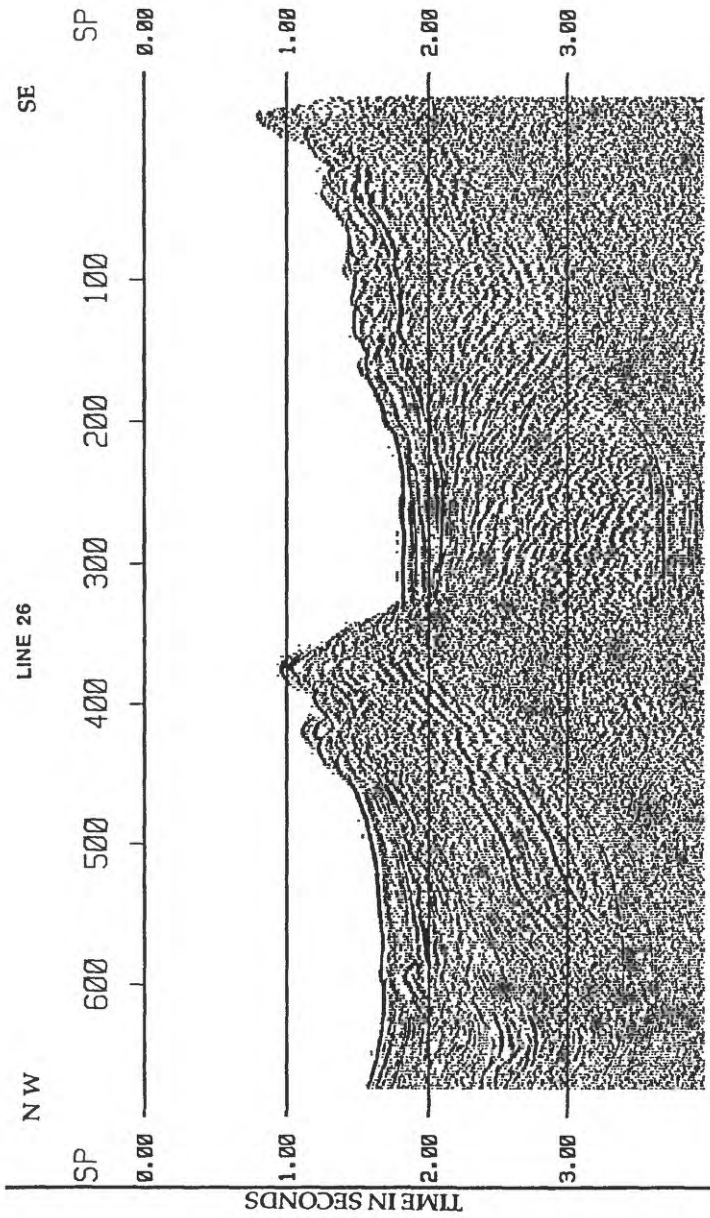
5-KM



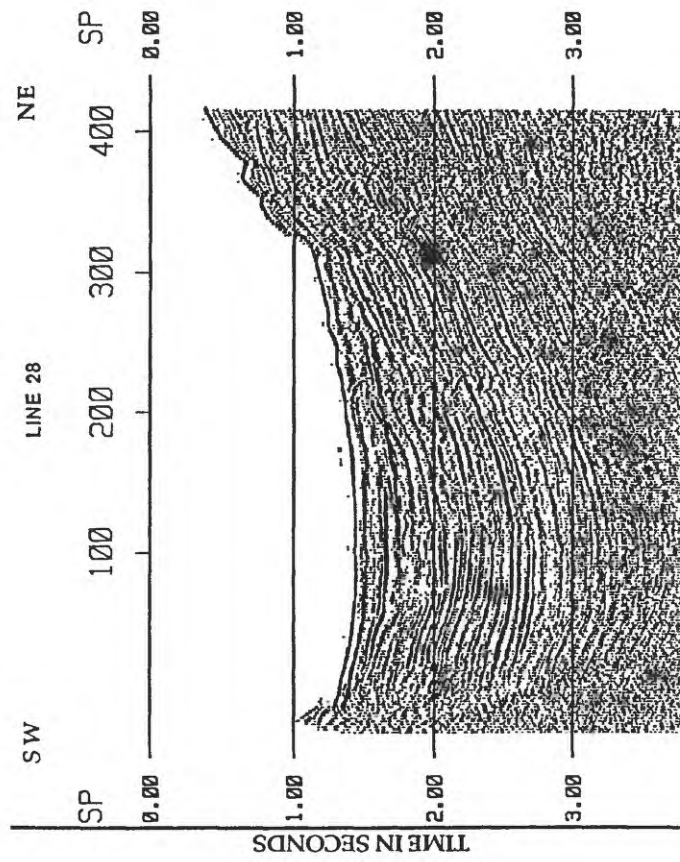


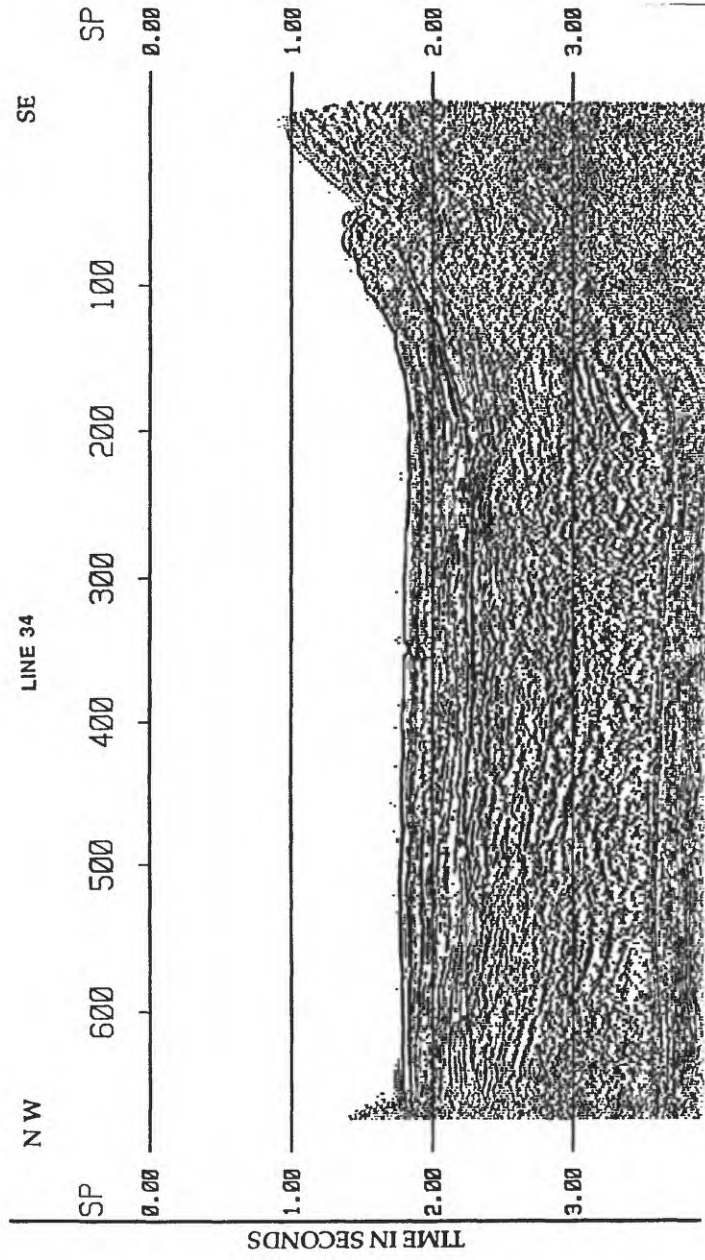
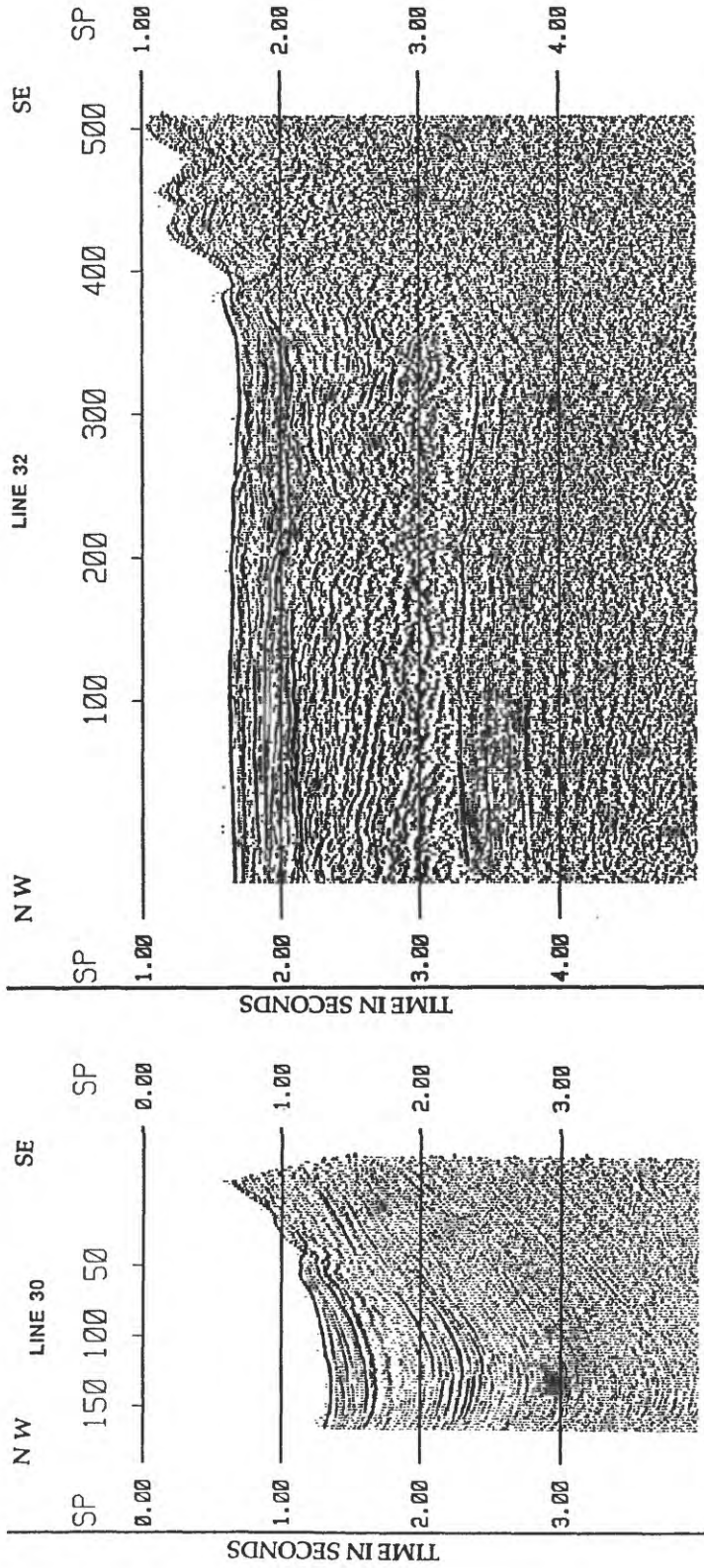
5-KM

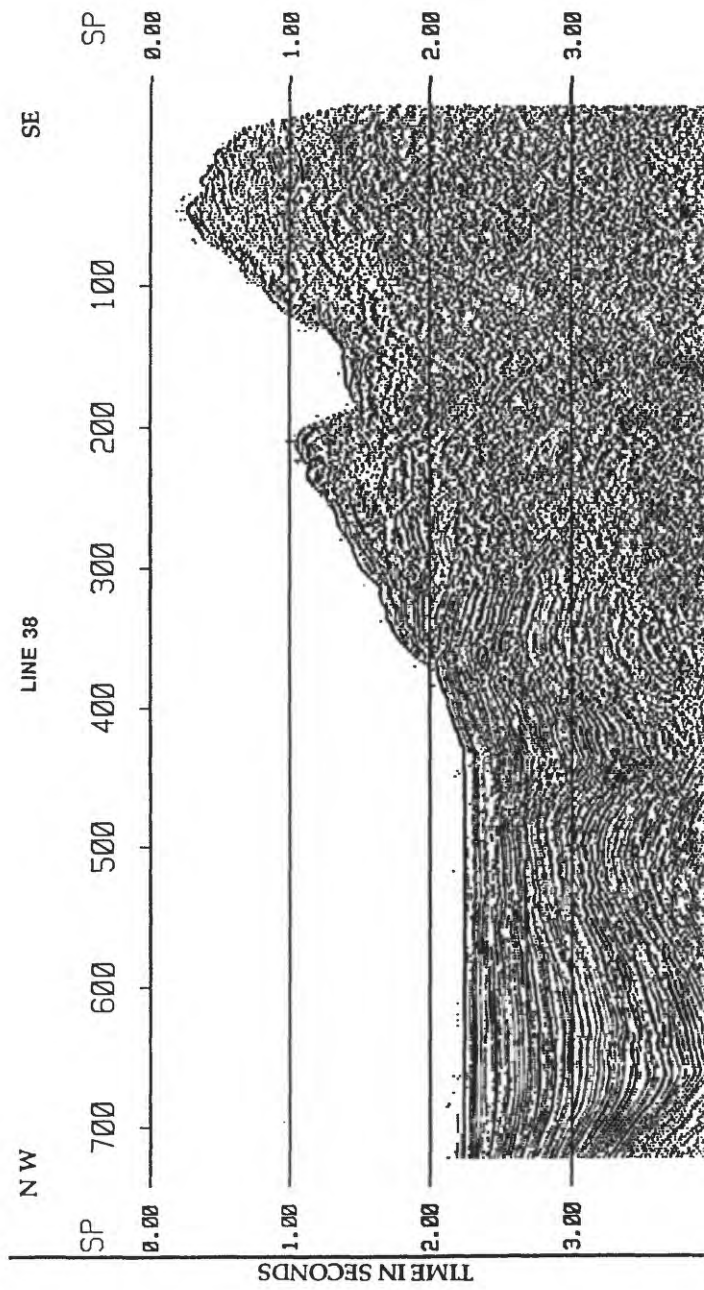
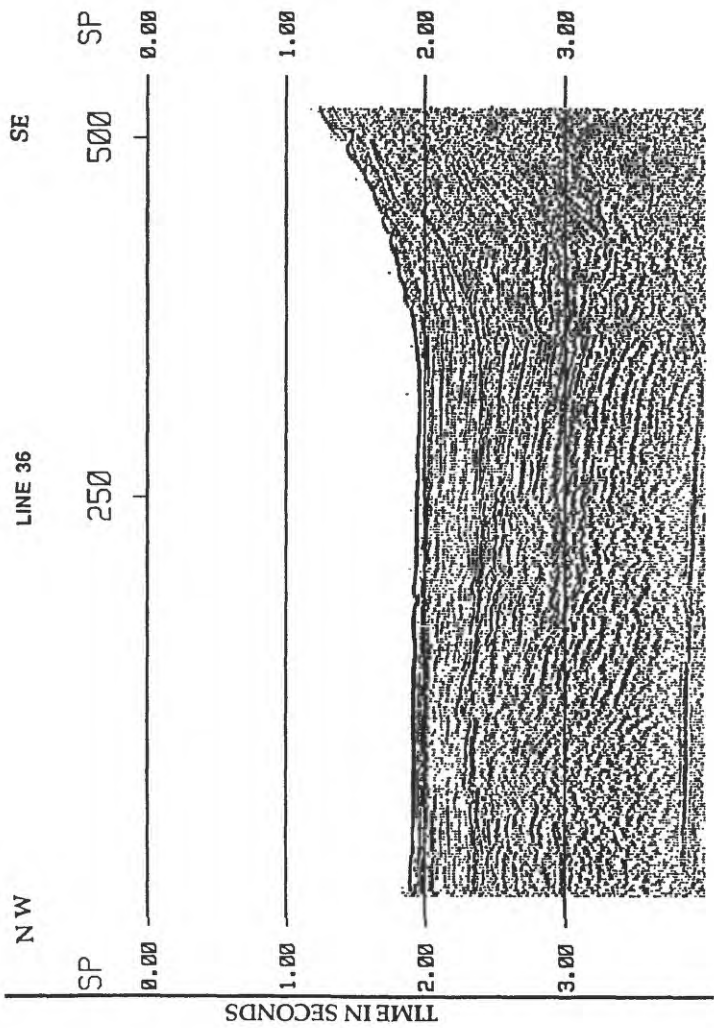


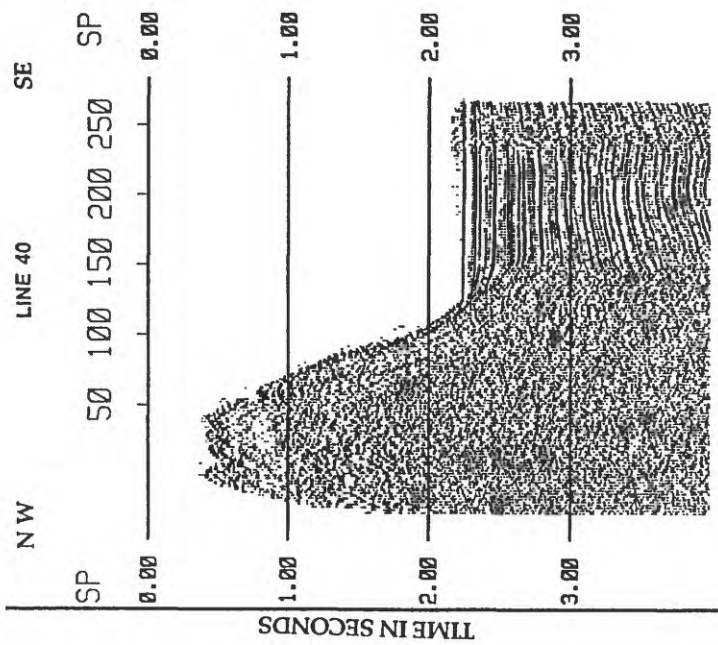


5-KM

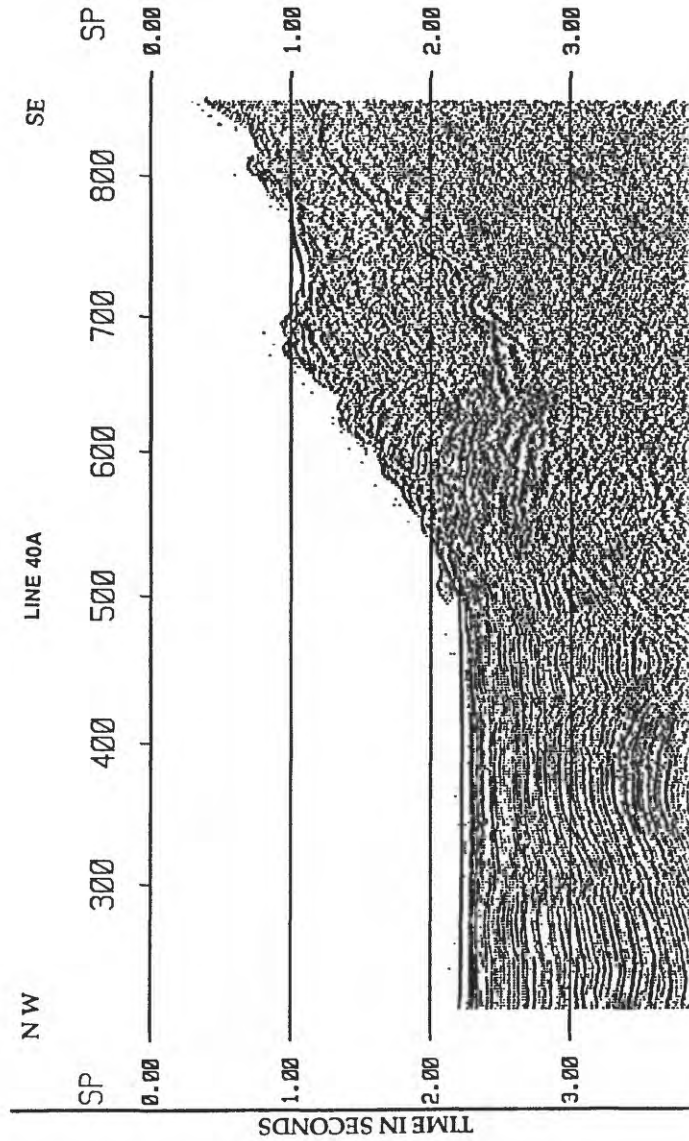


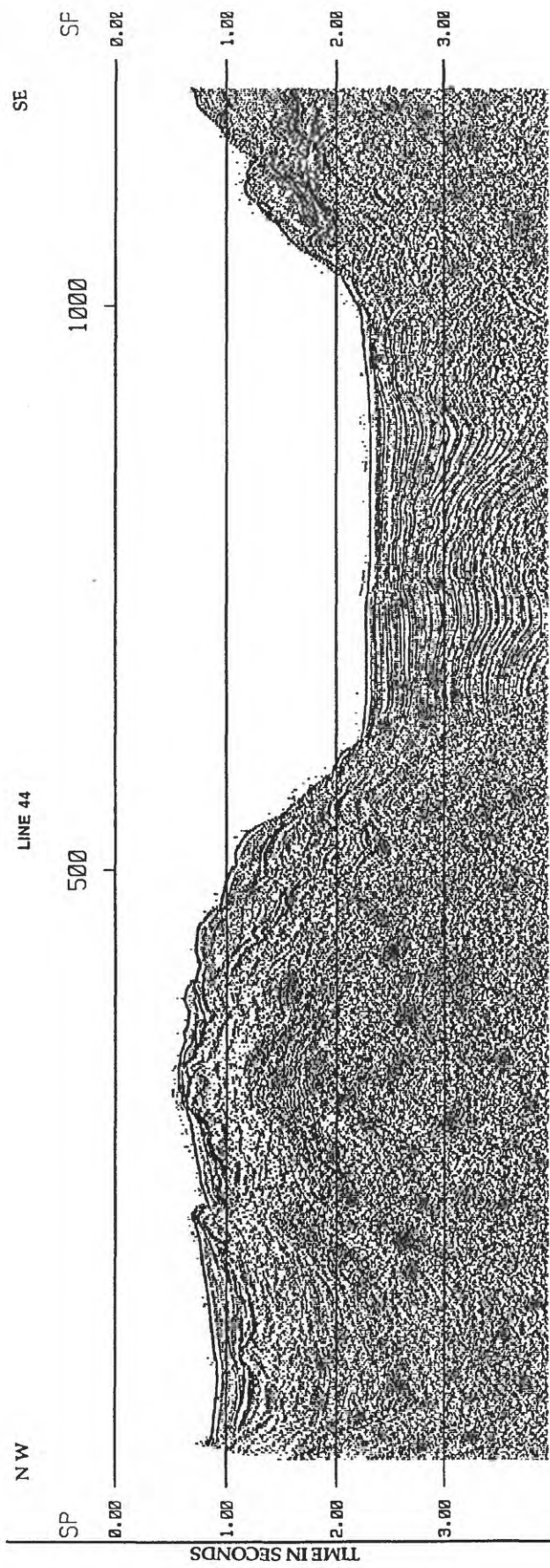
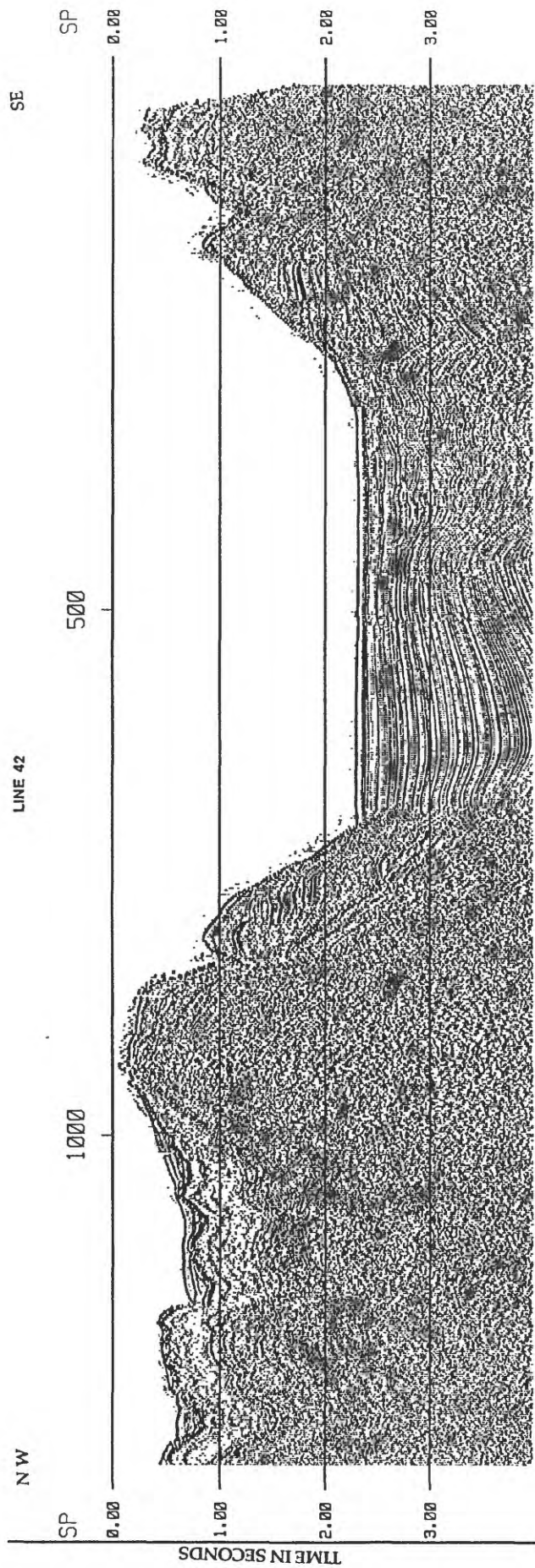


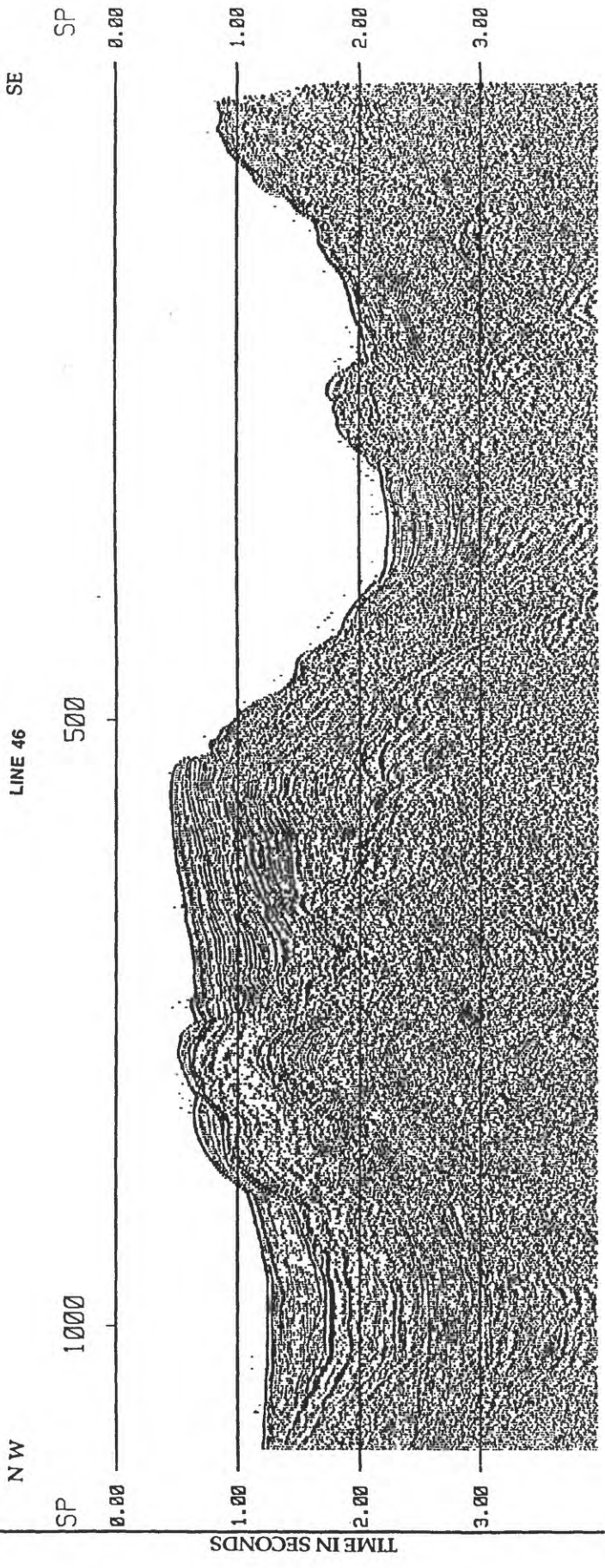




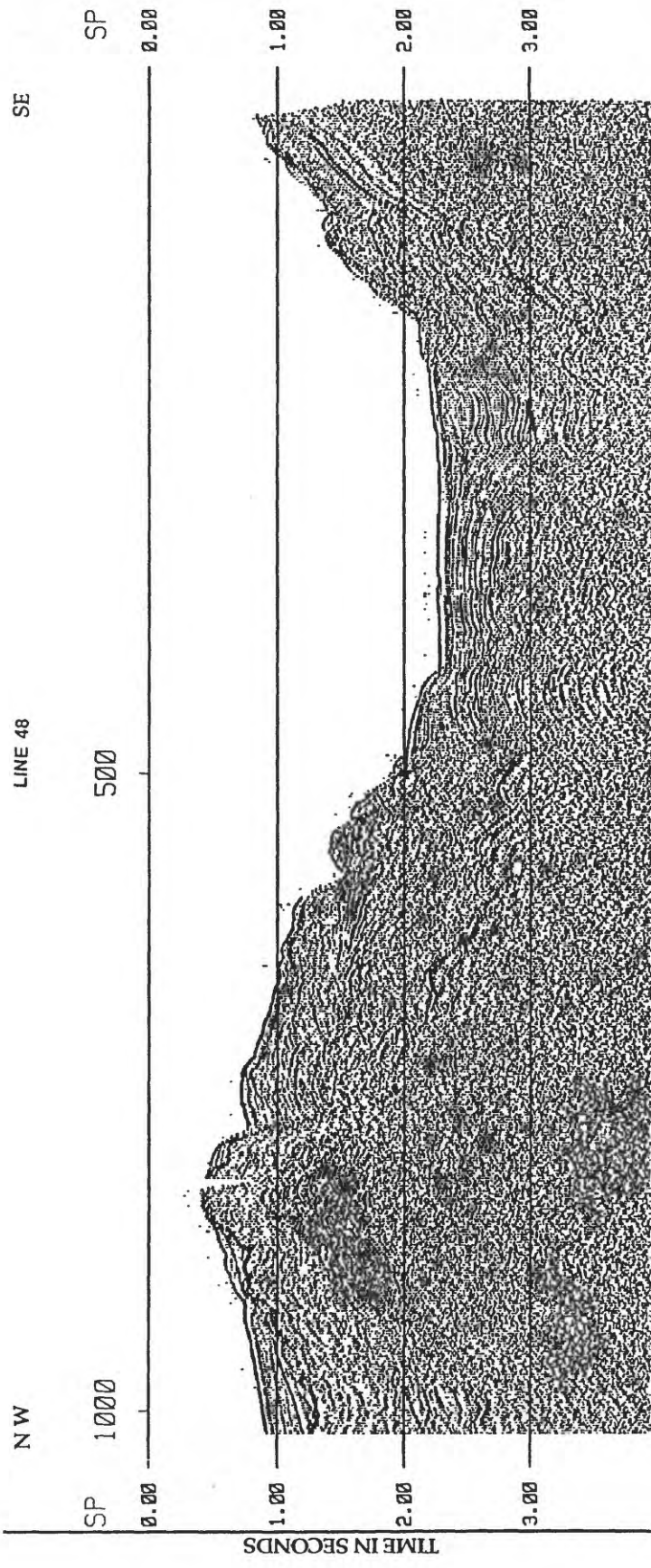
5-KM

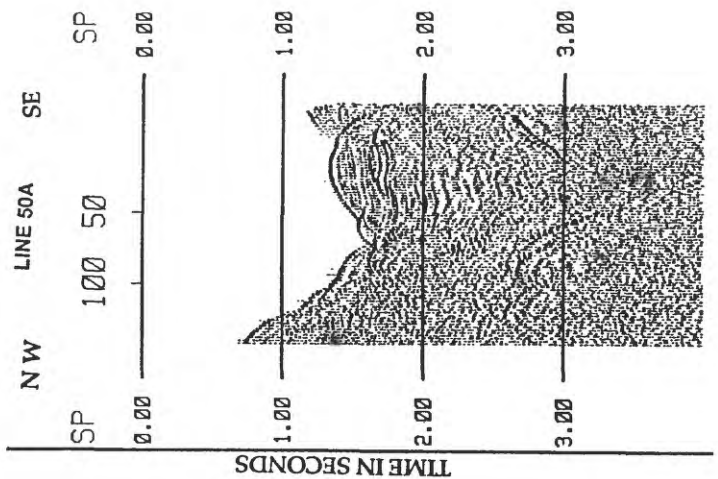
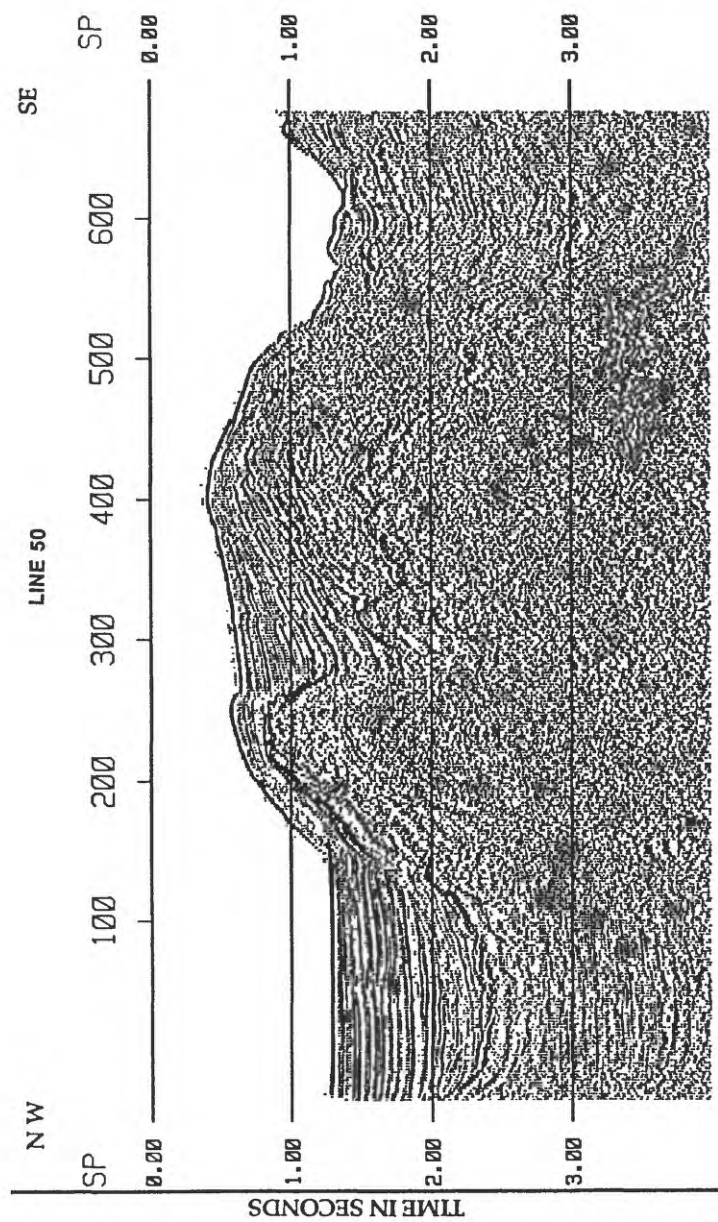




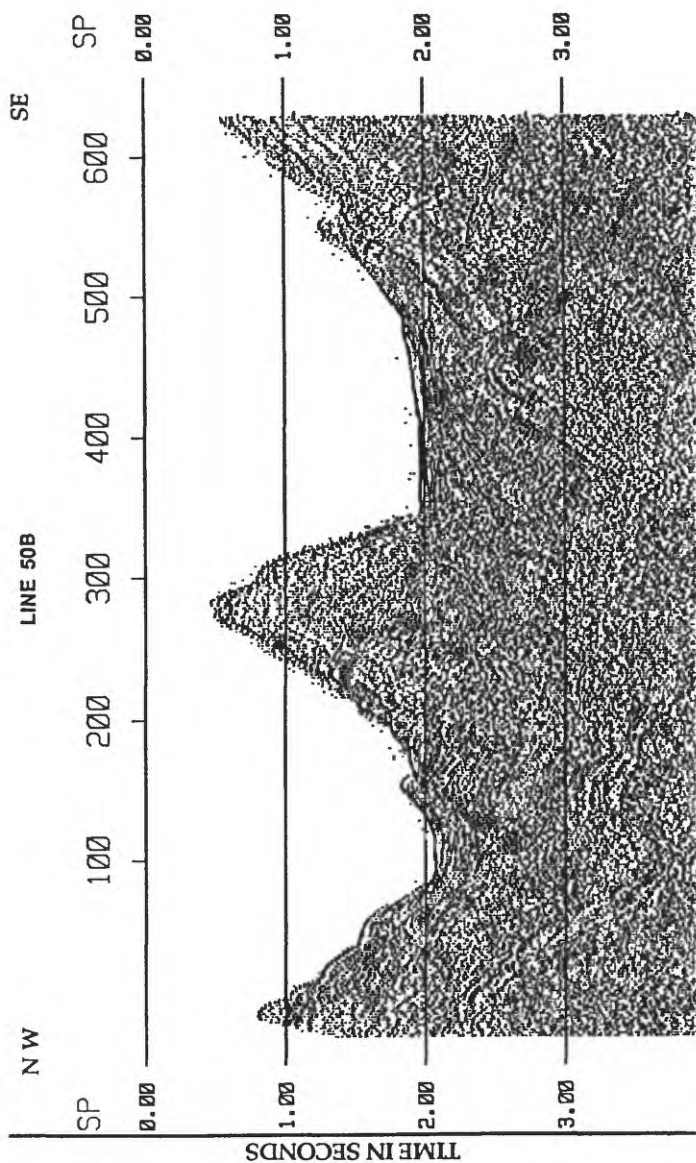


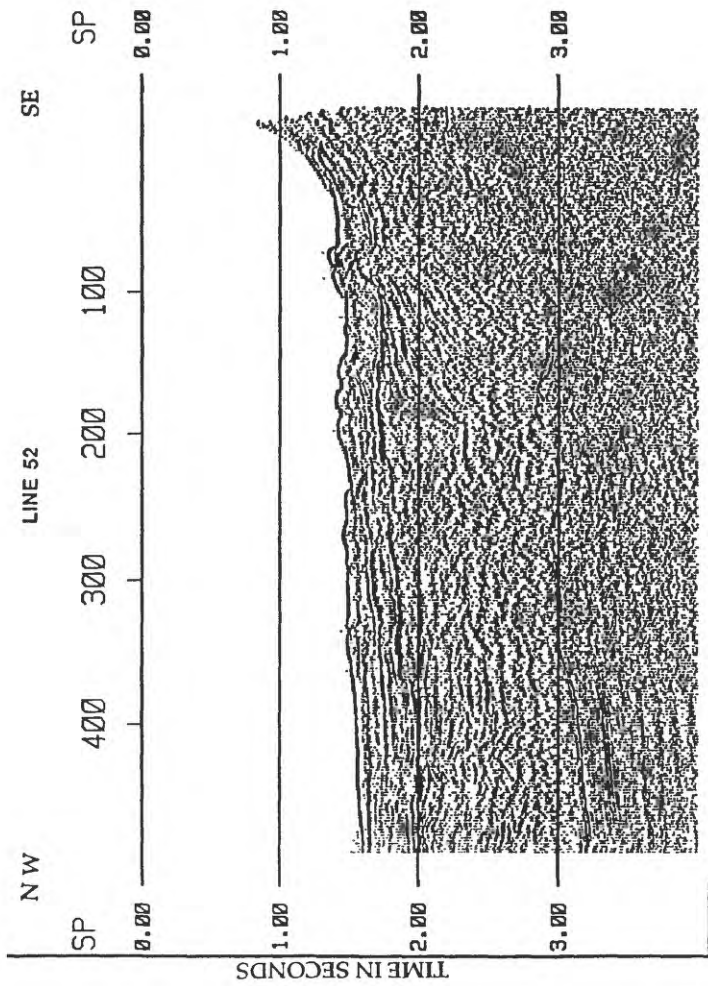
5-KM





5-KM





5-KM

